

# Enabling and Probing Oxidative Addition and Reductive Elimination at a Group 14 Metal Center: Cleavage and Functionalization of E–H Bonds by a Bis(boryl)stannylenes

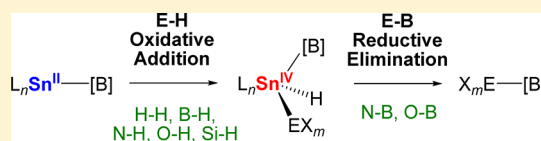
Andrey V. Protchenko,<sup>†</sup> Joshua I. Bates,<sup>†</sup> Liban M. A. Saleh,<sup>†</sup> Matthew P. Blake,<sup>†</sup> Andrew D. Schwarz,<sup>†</sup> Eugene L. Kolychov,<sup>†</sup> Amber L. Thompson,<sup>†</sup> Cameron Jones,<sup>‡</sup> Philip Mountford,<sup>†</sup> and Simon Aldridge<sup>\*,†</sup>

<sup>†</sup>Inorganic Chemistry Laboratory, Department of Chemistry, University of Oxford, South Parks Road, Oxford, OX1 3QR, U.K.

<sup>‡</sup>School of Chemistry, Monash University, PO Box 23, Melbourne, VIC 3800, Australia

## Supporting Information

**ABSTRACT:** By employing strongly  $\sigma$ -donating boryl ancillary ligands, the oxidative addition of  $H_2$  to a single site  $Sn^{II}$  system has been achieved for the first time, generating  $(boryl)_2SnH_2$ . Similar chemistry can also be achieved for protic and hydridic E–H bonds (N–H/O–H, Si–H/B–H, respectively). In the case of ammonia (and water, albeit more slowly), E–H oxidative addition can be shown to be followed by reductive elimination to give an N- (or O-)borylated product. Thus, in stoichiometric fashion, redox-based bond cleavage/formation is demonstrated for a single main group metal center at room temperature. From a mechanistic viewpoint, a two-step coordination/proton transfer process for N–H activation is shown to be viable through the isolation of species of the types  $Sn(boryl)_2 \cdot NH_3$  and  $[Sn(boryl)_2(NH_2)]^-$  and their onward conversion to the formal oxidative addition product  $Sn(boryl)_2(H)(NH_2)$ .



## INTRODUCTION

Oxidative addition and reductive elimination represent fundamental chemical steps familiar from undergraduate textbooks and key to numerous societally important catalytic processes.<sup>1</sup> The associated  $M^{n+}/M^{(n+2)+}$  redox shuttle, while facile for noble metals, is not well established for main group systems.<sup>2</sup> This reflects the fact that although oxidative bond activation by subvalent main group systems is well-known (e.g., for 6-valence-electron carbenes),<sup>3</sup> subsequent regeneration of the reduced state via reductive elimination is typically not thermodynamically viable.<sup>4</sup>

With reductive elimination in mind, one potential strategy is to target metallylenes featuring the heavier Group 14 elements, i.e., to exploit metals with intrinsically weaker M–E bonds (and a more favorable  $M^{II}/M^{IV}$  potential). The thermodynamic balance between facilitating reductive elimination and maintaining the capability for oxidative addition is a fine one, however; diarylgermylene systems ( $Ar_2Ge$ ) have been reported to react with E–H bonds via oxidative addition to give  $Ge^{IV}$  products, but the corresponding stannylenes react via a concerted exchange process, releasing arene and leading to the formation of  $Sn^{II}$  systems containing Sn–E linkages (E = H,  $NH_2$ , OR etc.).<sup>5–7</sup> To date—while addition to distannynes ( $R_2SnSnR$ ) has been reported—no experimental evidence exists for the oxidative addition of the archetypal E–H bond (i.e., that in  $H_2$ ) at a mononuclear  $Sn^{II}$  system to give the corresponding  $Sn^{IV}$  dihydride.<sup>6,7</sup>

We hypothesized that the  $Sn^{II}/Sn^{IV}$  redox couple might be manipulated to promote oxidative addition by the use of more strongly  $\sigma$ -donating ancillary ligands. Thus, given the fact that boryl ligands ( $-BX_2$ ) are known to be extremely strong  $\sigma$ -

donors (to greater extent even than hydride, alkyl or aryl donors),<sup>8</sup> we targeted oxidative bond activation by boryltin(II) systems.<sup>9</sup> In addition, with the kinetics of E–H oxidative addition in mind, it has been reported that the energy gap between the metallylene singlet ground state and triplet excited state ( $\Delta E_{st}$ ) is inversely correlated with reactivity.<sup>5a,10</sup> The very strong  $\sigma$ -donor capabilities of boryl substituents are hypothesized to raise the energy of the metallylene HOMO, and so reduce the HOMO/LUMO separation (and thus the related singlet–triplet gap).<sup>9a</sup> As such, from a kinetic as well as a thermodynamic perspective,  $(boryl)Sn^{II}$  systems were perceived as being potential candidates for the activation of E–H bonds.

In the current study we demonstrate that by targeted choice of ancillary substituents,  $Sn^{II}$  systems can be synthesized that are capable of a range of oxidative addition processes, relevant not only to  $H_2$ , but also to protic and hydridic E–H bonds. Mechanistically, through the isolation of potential intermediate species we establish experimentally the viability of a two-step activation process for ammonia, involving initial coordination at the metal center, followed by N-to-Sn proton transfer. In addition, in the cases of  $NH_3$  and  $H_2O$ , this net oxidative addition process can be shown to be followed by reductive elimination to give an N- (or O-)borylated product, thus providing demonstration (in stoichiometric fashion) of redox-based bond cleavage/formation at a main group metal.

Received: January 20, 2016

Published: March 16, 2016

## EXPERIMENTAL SECTION

**General Methods and Instrumentation.** All manipulations were carried out using standard Schlenk line or drybox techniques under an atmosphere of argon or dinitrogen. Solvents were degassed by sparging with dinitrogen and dried by passing through a column of the appropriate drying agent. THF was refluxed over potassium–sodium alloy and distilled prior to use. NMR spectra were measured in  $C_6D_6$  which was dried over potassium, distilled under reduced pressure and stored under dinitrogen in Teflon valve ampules. NMR samples were prepared under dinitrogen in 5 mm Wilmad 507-PP tubes fitted with J. Young Teflon valves.  $^1H$  and  $^{13}C\{^1H\}$  NMR spectra were recorded on Varian Mercury-VX 300 MHz, Bruker Avance III HD nanobay 400 MHz or Bruker Avance III 500 MHz spectrometer at ambient temperature unless stated otherwise and referenced internally to residual protiosolvent ( $^1H$ ) or solvent ( $^{13}C$ ) resonances and are reported relative to tetramethylsilane ( $\delta = 0$  ppm).  $^{11}B\{^1H\}$  NMR spectra were referenced to external  $Et_2O \cdot BF_3$ . Assignments were confirmed using two-dimensional  $^1H-^1H$  and  $^{13}C-^1H$  NMR correlation experiments. Chemical shifts are quoted in  $\delta$  (ppm) and coupling constants in Hz. Coupling to  $^{117/119}Sn$  nuclei was confirmed by measuring the spectrum of the same sample at a different spectrometer frequency. Elemental analyses were carried out by London Metropolitan University. Starting materials  $Sn\{B(NDippCH)_2\}_2$  (Dipp = 2,6- $C_6H_3Pr_2$ ) (**1**),  $Sn\{NDipp(SiMe_3)\}_2\{B(NDippCH)_2\}_2$  (**2**), and  $Si\{NDipp(SiMe_3)\}_2\{Si(SiMe_3)_3\}$  were synthesized according to published procedures.<sup>9a,11</sup> Silane was prepared in a similar manner to that described in ref 12 from  $SiCl_4$  (2.78 g, 16.3 mmol) and  $LiAlH_4$  (0.63 g, 16.6 mmol) in  $Et_2O$  (20 mL) in a degassed 400 mL ampule and used without fractionation (**Caution!**  $SiH_4$  reacts violently with air!). Ammonia was dried by condensing onto a Na mirror and distilling the required amount into a Young's tap ampule of such volume so that 1 atm pressure of  $NH_3$  was achieved at RT. Phenylsilane and  $BH_3 \cdot NMe_3$  (Aldrich) were carefully degassed and stored under a protective atmosphere.

**Syntheses of Novel Compounds.** Included here are synthetic and characterizing data for 3-9, 1-NH<sub>3</sub> and 1-NH<sub>2</sub>·Bu. The corresponding data for  $H_2NB(NDippCH)_2$ ,  $Sn\{B(NDippCH)_2\}_2Cl_2$ ,  $\{MeCCH_2\}_2\{Sn\{NDipp(SiMe_3)\}_2\{B(NDippCH)_2\}$  and  $Si\{Si(SiMe_3)_3\}\{N(SiMe_3)Dipp\}(H)(NH_2)$  are included in the Supporting Information. An alternative synthesis of  $H_2NB(NDippCH)_2$  has recently been reported.<sup>9c</sup> Reliable microanalytical data for intermediate compounds 1-NH<sub>3</sub>, 7 and 9 proved impossible to obtain because of their ready onward reactivity yielding  $H_2NB(NDippCH)_2$  and  $HB(NDippCH)_2$ .

$Sn\{B(NDippCH)_2\}_2H_2$ , **3**. A solution/suspension of **1** (137 mg, 0.153 mmol) in hexane (3 mL) was degassed by two freeze–pump–thaw cycles and exposed to 1 atm of  $H_2$  at 20 °C. The mixture was stirred at this temperature until the color had changed to pale brown (ca. 3 h). The mixture was filtered and concentrated to a small volume; crystallization was initiated by partial freezing with liquid  $N_2$  and continued at room temperature. The resulting colorless crystals were washed with a small amount of cold hexane and dried in vacuo yielding **3** (110 mg, 0.123 mmol, 80.3%). Anal. found (calcd. for  $C_{52}H_{74}B_2N_4Sn$ ): C, 69.64 (69.74); H, 8.26 (8.33); N, 6.23 (6.26) %.  $^1H$  NMR ( $C_6D_6$ ):  $\delta$  7.20 (4 H, t,  $^3J = 7.7$  Hz, *p*-H of Ar), 7.07 (8 H, d,  $^3J = 7.7$  Hz, *m*-H of Ar), 6.20 (4 H, s, with  $^{119/117}Sn$  satellites  $^4J(Sn-H) = 10$  Hz, NCH), 3.03 (8 H, septet,  $^3J = 6.9$  Hz,  $CHMe_2$ ), 2.22 (2 H, s, with  $^{119/117}Sn$  satellites  $^1J(^{119}Sn-^1H) = 1337$  and  $^1J(^{117}Sn-^1H) = 1277$  Hz,  $SnH_2$ ), 1.09 (24 H, d,  $^3J = 6.9$  Hz,  $CHMe_2$ ), 1.03 (24 H, d,  $^3J = 6.9$  Hz,  $CHMe_2$ ).  $^{13}C\{^1H\}$  NMR ( $C_6D_6$ ):  $\delta$  145.91 (*o*-C of Ar), 140.34 (*ipso*-C of Ar), 127.76 (*p*-CH of Ar), 123.64 (*m*-CH of Ar), 122.56 (s with  $^{119/117}Sn$  satellites  $^3J(Sn-H) = 34$  Hz, NCH), 28.71 ( $CHMe_2$ ), 25.37 ( $CHMe_2$ ), 23.73 ( $CHMe_2$ ).  $^{11}B\{^1H\}$  ( $C_6D_6$ ):  $\delta$  28.3. Crystallographic data (for **3**):  $C_{52}H_{74}B_2N_4Sn$ ,  $M_r = 895.50$ ,  $a = 12.6324(2)$  Å,  $b = 20.8368(3)$  Å,  $c = 19.7169(3)$  Å,  $\beta = 95.4397(14)^\circ$ , monoclinic,  $P2_1/c$ ,  $V = 5166.51(14)$  Å<sup>3</sup>,  $Z = 4$ ,  $R_1$  for 9810 [data intensity  $I > 2\sigma(I)$ ] unique reflections = 0.0390,  $wR_2$  (all 10686 unique reflections) = 0.0395. CCDC ref: 1055214.

$Sn\{B(NDippCH)_2\}_2(H)(SiH_3)$ , **4a**. A degassed solution of **1** (95 mg, 0.106 mmol) in  $C_6H_6$  (2 mL) was exposed to an atmosphere of silane. After 5 min of stirring at 20 °C the yellow-green color disappeared, all volatiles were removed in vacuo and the residue was extracted with hexane (3 × 5 mL). The extract was evaporated to dryness, and the resulting light-brown solid washed with a small amount of cold hexane and dried in vacuo yielding colorless crystalline **4a** (76 mg, 0.082 mmol, 77.5%). Anal. found (calcd. for  $C_{52}H_{76}B_2N_4SiSn$ ): C, 67.65 (67.48); H, 8.38 (8.28); N, 6.21 (6.05) %.  $^1H$  NMR ( $C_6D_6$ ):  $\delta$  7.19 (4 H, t,  $^3J = 7.7$  Hz, *p*-H of Ar), 7.09 (8 H, d,  $^3J = 7.7$  Hz, *m*-H of Ar), 6.16 (4 H, s, with  $^{119/117}Sn$  satellites  $^4J(Sn-H) = 9.5$  Hz, NCH), 3.21 (4 H, septet,  $^3J = 6.83$  Hz,  $CHMe_2$ ), 2.92 (4 H, septet,  $^3J = 6.83$  Hz,  $CHMe_2$ ), 2.27 (3 H, d,  $^3J = 3.83$  Hz, with  $^{119/117}Sn$  satellites  $^2J(Sn-H) = 39.9$  Hz and  $^{29}Si$  satellites  $^1J(Si-H) = 191.2$  Hz,  $SiH_3$ ), 1.66 (1 H, quartet,  $^3J = 3.83$  Hz, with  $^{119/117}Sn$  satellites  $^1J(Sn-H) = 1223$  and 1281 Hz,  $SnH$ ), 1.06–1.13 (48 H, four overlapping doublets,  $CHMe_2$ ).  $^{13}C\{^1H\}$  NMR ( $C_6D_6$ ):  $\delta$  146.17 (*o*-C of Ar), 145.74 (*o*-C of Ar), 140.61 (*ipso*-C of Ar), 127.93 (*p*-CH of Ar), 124.28 (*m*-CH of Ar), 123.73 (*m*-CH of Ar), 123.28 ( $^{119/117}Sn$  satellites  $^3J(Sn-C) = 32.9$  Hz, NCH), 28.92 ( $CHMe_2$ ), 28.47 ( $CHMe_2$ ), 25.96 ( $CHMe_2$ ), 25.89 ( $CHMe_2$ ), 24.31 ( $CHMe_2$ ), 22.80 ( $CHMe_2$ ).  $^{11}B\{^1H\}$  ( $C_6D_6$ ):  $\delta$  27.9.  $^{29}Si\{^1H\}$  ( $C_6D_6$ ):  $\delta$  -108.8.

$Sn\{B(NDippCH)_2\}_2(H)(SiH_2Ph)$ , **4b**. Phenylsilane (10.8 mg, 12.3  $\mu$ L, 0.10 mmol) was added to a solution of **1** (75 mg, 0.084 mmol) in  $C_6D_6$  (0.7 mL). Almost immediately the yellow-green color disappeared and  $^1H$  NMR spectrum showed clean formation of a single product (excess  $PhSiH_3$  was also present). The mixture was transferred into a two-section crystallization tube and volatiles removed in vacuo. The residue was dissolved in hexane (1 mL) and the tube sealed under a vacuum. The solution was slowly concentrated at room temperature while large colorless blocks formed. The resulting crystals were washed with a small amount of cold hexane and dried in vacuo yielding **4b** (59 mg, 0.059 mmol, 70.1%). Anal. found (calcd. for  $C_{58}H_{80}B_2N_4SiSn$ ): C, 69.79 (69.54); H, 8.18 (8.05); N, 5.47 (5.59) %.  $^1H$  NMR ( $C_6D_6$ ):  $\delta$  7.36 (2 H, m, *o*-H of Ph), 7.21 (4 H, t,  $^3J = 7.7$  Hz, *p*-H of Ar), 7.05–7.11 (8 + 3 H, m, *m*-H of Ar and *m*- and *p*-H of Ph), 6.15 (4 H, s, with  $^{119/117}Sn$  satellites  $^4J(Sn-H) = 9.4$  Hz, NCH), 3.86 (2 H, d,  $^3J = 3.69$  Hz, with  $^{119/117}Sn$  satellites  $^2J(Sn-H) = 64.5$  Hz and  $^{29}Si$  satellites  $^1J(Si-H) = 190.3$  Hz,  $SiH_2Ph$ ), 3.17 (4 H, septet,  $^3J = 6.88$  Hz,  $CHMe_2$ ), 2.96 (4 H, septet,  $^3J = 6.88$  Hz,  $CHMe_2$ ), 1.84 (1 H, t,  $^3J = 3.69$  Hz, with  $^{119/117}Sn$  satellites  $^1J(Sn-H) = 1197$  and 1252 Hz,  $SnH$ ), 1.12 (12 H, d,  $^3J = 6.88$  Hz,  $CHMe_2$ ), 1.08 (12 H, d,  $^3J = 6.88$  Hz,  $CHMe_2$ ), 1.03 (12 H, d,  $^3J = 6.88$  Hz,  $CHMe_2$ ), 0.94 (12 H, d,  $^3J = 6.88$  Hz,  $CHMe_2$ ).  $^{13}C\{^1H\}$  NMR ( $C_6D_6$ ):  $\delta$  146.30 (*o*-C of Ar), 145.91 (*o*-C of Ar), 140.86 (*ipso*-C of Ar), 137.19 ( $^{119/117}Sn$  satellites  $^3J(Sn-C) = 12.9$  Hz, *o*-CH of Ph), 133.18 ( $^{119/117}Sn$  satellites  $^2J(Sn-C) = 8.6$  Hz, *ipso*-C of Ph), 128.75 (*p*-CH of Ph), 127.94 (*p*-CH of Ar), 127.61 (*m*-CH of Ph), 124.25 (*m*-CH of Ar), 123.75 (*m*-CH of Ar), 123.57 ( $^{119/117}Sn$  satellites  $^3J(Sn-C) = 32.6$  Hz, NCH), 28.91 ( $CHMe_2$ ), 28.44 ( $CHMe_2$ ), 26.11 ( $CHMe_2$ ), 25.96 ( $CHMe_2$ ), 24.07 ( $CHMe_2$ ), 23.00 ( $CHMe_2$ ).  $^{11}B\{^1H\}$  ( $C_6D_6$ ):  $\delta$  28.1.  $^{29}Si\{^1H\}$  ( $C_6D_6$ ):  $\delta$  -63.1 (with  $^{119/117}Sn$  satellites  $^1J(Sn-Si) = 409.4$  and 428.5 Hz). Crystallographic data (for **4b**):  $C_{58}H_{80}B_2N_4SiSn$ ,  $M_r = 1001.79$ ,  $a = 12.5270(4)$  Å,  $b = 12.6173(5)$  Å,  $c = 21.1768(8)$  Å,  $\alpha = 79.505(3)^\circ$ ,  $\beta = 89.404(3)^\circ$ ,  $\gamma = 60.709(4)^\circ$ , triclinic,  $\bar{P}1$ ,  $V = 2858.2(2)$  Å<sup>3</sup>,  $Z = 2$ ,  $R_1$  for 10834 [data intensity  $I > 2\sigma(I)$ ] unique reflections = 0.0614,  $wR_2$  (all 11774 unique reflections) = 0.0767. CCDC ref: 1055215.

$Sn\{B(NDippCH)_2\}_2(H)(BH_2 \cdot NMe_3)$ , **5**. Trimethylamine borane (7.3 mg, 0.10 mmol) was added to a solution of **1** (102 mg, 0.114 mmol) in  $C_6H_6$  (2 mL). A preliminary NMR-monitored experiment showed that no apparent reaction occurred at room temperature, but the starting stannylene was consumed after 11 h at 50 °C. Accordingly, on a preparative scale, the reaction mixture was heated overnight at 50 °C producing a light brown solution. The mixture was then transferred into a two-section crystallization tube and all volatiles removed in vacuo. Hexane (2 mL) was added to the residue and the tube was sealed under a vacuum. Crystallization by slow evaporation at room temperature gave colorless crystals contaminated with a brown powder. The product was recrystallized again by extraction with

warm hexane and storing the concentrated extract at 4 °C. This yielded clear blocks, which were washed with a small amount of cold hexane and dried in vacuo turning into a white powder (26 mg, 0.027 mmol, 23.5%). Anal. found (calcd. for  $C_{55}H_{84}B_3N_5Sn$ ): C, 68.51 (68.35); H, 8.92 (8.76); N, 7.16 (7.25)%.  $^1H$  NMR ( $C_6D_6$ ):  $\delta$  7.21 (4 H, t,  $^3J = 7.4$  Hz, *p*-H of Ar), 7.16 (8 H, d,  $^3J = 7.4$  Hz, *m*-H of Ar +  $C_6D_5H$ ), 6.22 (4 H, s, with  $^{119/117}Sn$  satellites  $^4J(Sn-H) = 6.5$  Hz, NCH), 3.30 (4 H, septet,  $^3J = 6.83$  Hz,  $CHMe_2$ ), 3.17 (4 H, septet,  $^3J = 6.83$  Hz,  $CHMe_2$ ), 2.14 (2 H, br s,  $BH_2$ ), 1.73 (9 H, s,  $NMe_3$ ), 1.12–1.21 (48 H, four overlapping doublets,  $CHMe_2 + CH_2$  of hexane), 1.11 (1 H, br s, with  $^{119/117}Sn$  satellites  $^1J(Sn-H) = 893.9$  and  $936.2$  Hz, SnH), 0.88 (6 H, t, Me of hexane).  $^{13}C\{^1H\}$  NMR ( $C_6D_6$ ):  $\delta$  146.71 (*o*-C of Ar), 146.54 (*o*-C of Ar), 142.22 (*ipso*-C of Ar), 127.19 (*p*-CH of Ar), 123.86 (*m*-CH of Ar), 123.78 (*m*-CH of Ar), 123.05 ( $^{119/117}Sn$  satellites  $^3J(Sn-C) = 24.2$  Hz, NCH), 54.42 ( $^{119/117}Sn$  satellites  $^3J(Sn-C) = 36.3$  Hz,  $NMe_3$ ), 31.92 ( $CH_2$  of hexane), 28.57 ( $CHMe_2$ ), 28.53 ( $CHMe_2$ ), 26.82 ( $CHMe_2$ ), 26.35 ( $CHMe_2$ ), 23.76 ( $CHMe_2$ ), 23.48 ( $CHMe_2$ ), 23.01 ( $CH_2$  of hexane), 14.31 (Me of hexane).  $^{11}B\{^1H\}$  ( $C_6D_6$ ):  $\delta$  31.9 (3-coordinate boryl), – 8.26 ( $BH_2NMe_3$ ). Crystallographic data (for **5**):  $C_{55}H_{84}B_3N_5Sn$ ,  $M_r = 966.43$ ,  $a = 14.1360(2)$  Å,  $b = 16.8914(2)$  Å,  $c = 25.9133(4)$  Å,  $\beta = 99.1667(12)^\circ$ , monoclinic,  $P2_1/c$ ,  $V = 6108.47(15)$  Å<sup>3</sup>,  $Z = 4$ ,  $R_1$  for 12064 [data intensity  $I > 2\sigma(I)$ ] unique reflections = 0.0412,  $wR_2$  (all 12712 unique reflections) = 0.0505. CCDC ref: 1055216.

$Sn\{B(NDippCH)_2\}_2(H)(OH)$ , **6**. To a solution of **1** (108 mg, 0.121 mmol) in  $C_6H_6$  (2 mL) was added dropwise wet benzene (prepared by stirring dry, deoxygenated benzene (20 mL) with excess water (1 mL)) until the color change from yellow-green to light brown was complete (ca. 9 mL). All volatiles were removed in vacuo and the residue was dried for 2 h at 20 °C. The solid was redissolved in dry benzene and the solution was filtered to remove cloudiness. The resulting filtrate was slowly evaporated almost to dryness, while large colorless blocks were growing, and stored overnight at 4 °C to complete crystallization. Washing with a small amount of cold benzene and drying in vacuo yielded **6** (93.7 mg, 0.102 mmol, 85%). Anal. found (calcd. for  $C_{52}H_{74}B_2N_4OSn$ ): C, 68.66 (68.52); H, 8.28 (8.18); N, 6.16 (6.15)%. Compound **6** is only sparingly soluble in hexane and, when heated to reflux, reacted to give  $HB(NDippCH)_2$ ,  $HOB(NDippCH)_2$  and tin metal; thus X-ray quality crystals were obtained from methylcyclohexane at 4 °C.  $^1H$  NMR ( $C_6D_6$ ):  $\delta$  7.18 (4 H, t,  $^3J = 7.7$  Hz, *p*-H of Ar), 7.15 (s,  $C_6H_6$ ), 7.07 (8 H, m, *m*-H of Ar), 6.16 (4 H, s, with  $^{119/117}Sn$  satellites  $^4J(Sn-H) = 10.8$  Hz, NCH), 6.13 (br s, with  $^{119/117}Sn$  satellites  $^1J(Sn-H) = 1385$  and  $1450$  Hz, SnH), 3.17 (4 H, septet,  $^3J = 6.85$  Hz,  $CHMe_2$ ), 3.05 (4 H, septet,  $^3J = 6.85$  Hz,  $CHMe_2$ ), 1.10 (24 H, d,  $^3J = 6.85$  Hz,  $CHMe_2$ ), 1.09 (12 H, d,  $^3J = 6.85$  Hz,  $CHMe_2$ ), 1.06 (12 H, d,  $^3J = 6.85$  Hz,  $CHMe_2$ ), – 2.09 (1 H, d,  $^3J = 1.43$  Hz, with  $^{119/117}Sn$  satellites  $^2J(Sn-H) = 24.6$  Hz, SnOH).  $^{13}C\{^1H\}$  NMR ( $C_6D_6$ ):  $\delta$  146.30 (*o*-C of Ar), 145.94 (*o*-C of Ar), 139.77 (*ipso*-C of Ar), 128.53 ( $C_6H_6$ ), 128.00 (*p*-CH of Ar), 123.80 (*m*-CH of Ar), 123.69 (*m*-CH of Ar), 122.89 ( $^{119/117}Sn$  satellites  $^3J(Sn-C) = 38.1$  Hz, NCH), 28.77 ( $CHMe_2$ ), 28.66 ( $CHMe_2$ ), 25.56 ( $CHMe_2$ ), 25.45 ( $CHMe_2$ ), 23.95 ( $CHMe_2$ ), 23.61 ( $CHMe_2$ ).  $^{11}B\{^1H\}$  ( $C_6D_6$ ):  $\delta$  29.8. Crystallographic data (for **6**):  $C_{52}H_{74}B_2N_4OSn$ ,  $M_r = 911.48$ ,  $a = 21.22087(16)$  Å,  $b = 12.54026(11)$  Å,  $c = 19.63737(17)$  Å,  $\beta = 97.8858(8)^\circ$ , monoclinic,  $P2_1/c$ ,  $V = 5176.39(7)$  Å<sup>3</sup>,  $Z = 4$ ,  $R_1$  for 10463 [data intensity  $I > 2\sigma(I)$ ] unique reflections = 0.0491,  $wR_2$  (all 10735 unique reflections) = 0.0464. CCDC ref: 1055217.

$Sn\{B(NDippCH)_2\}_2(NH_3)$ , **1-NH<sub>3</sub>**. (i). Bulk Material. Compound **1** (265 mg, 0.297 mmol) was dissolved/suspended in hexane (5 mL), degassed by three freeze–pump–thaw cycles and cooled to 0 °C. When exposed to an atmosphere of dry ammonia, the yellow-green solution turned orange and undissolved crystals of **1** disappeared over a period of ca. 1 min, while small orange crystals of the product began to appear on the walls of the ampule. After stirring for a further 10 min the ampule was carefully opened to vacuum and the solvent and excess ammonia removed under reduced pressure, yielding light orange microneedles.  $^1H$  NMR ( $C_6D_6$ ) showed almost quantitative conversion into **1-NH<sub>3</sub>** at this point, and as recrystallization (from either hexane, pentane or cyclohexane) on a preparative scale requires

very careful handling (prolonged manipulation in solution results in decomposition) this product was typically used in further reactions as is.

(ii). Single Crystals. A degassed solution of **1** (50 mg, 0.056 mmol) in  $C_6H_6$  (1 mL) was exposed to an atmosphere of ammonia and shaken by hand until the color changed from yellow-green to bright orange (ca. 1 min). Volatiles were removed in vacuo and the residue extracted with *n*-hexane. The extract was then concentrated until the onset of crystallization and stored at 4 °C to produce large red-orange blocks of **1-NH<sub>3</sub>** suitable for X-ray diffraction. Further concentration and storage of the mother liquor produced a second crop of slightly less pure compound (total: 33 mg, 0.036 mmol, 65%).  $^1H$  NMR ( $C_6D_5CD_3$ , ref.: internal  $SiMe_4$ ):  $\delta$  7.06 (4 H, t,  $^3J = 7.6$  Hz, *p*-H of Ar), 6.97 (8 H, d,  $^3J = 7.6$  Hz, *m*-H of Ar), 6.25 (4 H, s, NCH), 3.62 (4 H, br,  $CHMe_2$ ), 3.25 (4 H, br,  $CHMe_2$ ), 1.11 (48 H, br,  $CHMe_2$ ), 0.27 (3 H, br s,  $NH_3$ ).  $^{13}C\{^1H\}$  NMR ( $C_6D_5CD_3$ , ref.: internal  $SiMe_4$ ):  $\delta$  146.47 (br, *o*-C of Ar), 142.02 (*ipso*-C of Ar), 127.29 (*p*-CH of Ar), 124.07 (br, *m*-CH of Ar), 122.82 (NCH), 28.77 ( $CHMe_2$ ), 25.79 (br,  $CHMe_2$ ), 23.95 (v br,  $CHMe_2$ ).  $^{11}B\{^1H\}$  ( $C_6D_5CD_3$ ):  $\delta$  45.1. Crystallographic data (for **1-NH<sub>3</sub>**):  $C_{52}H_{74}B_2N_5Sn$ ,  $M_r = 909.50$ ,  $a = 19.4712(2)$  Å,  $b = 14.5386(2)$  Å,  $c = 18.7150(2)$  Å,  $\beta = 105.3864(5)^\circ$ , monoclinic,  $P2_1/c$ ,  $V = 5108.04(5)$  Å<sup>3</sup>,  $Z = 4$ ,  $R_1$  for 9836 [data intensity  $I > 2\sigma(I)$ ] unique reflections = 0.0475,  $wR_2$  (all 11614 unique reflections) = 0.1302. CCDC ref: 1055211.

Onward Reaction of **1-NH<sub>3</sub>**. A sample of **1-NH<sub>3</sub>** was monitored by in situ multinuclear NMR spectroscopy while maintained at 20 °C for 4–5 days, revealing the formation of two metal-free products: the known compound  $HB(NDippCH)_2$ ,<sup>13</sup> and  $H_2NB(NDippCH)_2$  (identified by comparison of its  $^1H$  NMR spectral signals with those of independently prepared sample (see SI)). Although tin metal was also observed to be formed, we were also able to isolate small (but reproducible) quantities of a tin cluster species identified solely on the basis of X-ray crystallography as *nido*- $Sn_{11}\{B(NDippCH)_2\}_4$  and *nido*- $Sn_{10}\{B(NDippCH)_2\}_4$ . NMR monitoring further shows that the onward reaction of **1-NH<sub>3</sub>** proceeds via an intermediate (which achieves maximum concentration after ca. 2 d), identified as  $Sn\{B(NDippCH)_2\}_2(H)(NH_3)$  (**7**) through comparison of its Sn–H and Sn– $NH_2$   $^1H$  NMR signals with an authentic sample (prepared as outlined below). After 5 d no residual signals of **1-NH<sub>3</sub>** were observed in  $^1H$  NMR spectrum, and volatiles were removed in vacuo; the residue was extracted with hexane (1 mL) into a crystallization tube to remove the black precipitate of tin metal. The resulting solution was concentrated and stored at 4 °C for 2 d producing a very small quantity of black (brown in thin layer) block-like crystals of distorted hexagonal shape (1:4 mixture of  $Sn_{10}/Sn_{11}$  clusters). Similar (by X-ray diffraction) crystals were isolated reproducibly from three different experiments in very low yield. Further crystallization at –30 °C gave needle crystals containing both  $HB(NDippCH)_2$  and  $H_2NB(NDippCH)_2$ .

$Sn\{B(NDippCH)_2\}_2(^tBuNH_2)$ , **1-<sup>t</sup>BuNH<sub>2</sub>**. To a solution of **1** (27 mg, 0.030 mmol) in  $C_6H_6$  (1 mL) was added excess  $^tBuNH_2$  (10  $\mu$ L, 7.0 mg, 0.096 mmol) resulting in immediate color change from yellow-green to bright orange. Volatiles were removed in vacuo, the residue was extracted with *n*-hexane, the extract was concentrated to an oily drop which was stored in a fridge (4 °C) for several days producing large orange blocks of **1-<sup>t</sup>BuNH<sub>2</sub>** suitable for X-ray diffraction (after drying in vacuo became nontransparent; 14 mg, 0.014 mmol, 48%). Anal. found (calcd. for  $C_{56}H_{88}B_2N_5Sn$ ): C, 69.26 (69.58); H, 8.20 (8.66); N, 7.31 (7.25)%. The product is extremely sensitive toward hydrolysis by traces of water absorbed on glass surfaces (much more so than the starting material **1**) leading to contamination by **6** and  $HOB(NDippCH)_2$ .  $^1H$  NMR ( $C_6D_6$ ):  $\delta$  7.15 (4 H, m, *p*-H of Ar +  $C_6D_5H$ ), 7.08 (8 H, d,  $^3J = 7.7$  Hz, *m*-H of Ar), 6.32 (4 H, s, NCH), 3.28–3.67 (8 H, br,  $CHMe_2$ ), 1.79 (2 H, br s,  $NH_2$ ), 1.15 (48 H, br,  $CHMe_2$ ), 0.56 (9 H, s,  $CM_3$ ).  $^{13}C\{^1H\}$  NMR ( $C_6D_6$ ):  $\delta$  146.52 (*o*-C of Ar), 142.17 (*ipso*-C of Ar), 127.41 (*p*-CH of Ar), 124.33 (*m*-CH of Ar), 123.50 (NCH), 49.09 ( $CM_3$ ), 28.77 ( $CHMe_2$ ), 28.73 ( $CM_3$ ), 26.49 ( $CHMe_2$ ), 23.76 (v br,  $CHMe_2$ ).  $^{11}B\{^1H\}$  ( $C_6D_6$ ):  $\delta$  45.7. Crystallographic data (for **1-<sup>t</sup>BuNH<sub>2</sub>** (0.25  $C_6H_{14}$ )):  $C_{57.5}H_{86.5}B_2N_5Sn$ ,  $M_r = 988.16$ ,  $a = 20.3402(2)$  Å,  $b = 12.83950(10)$  Å,  $c = 22.8290(3)$  Å,

$\beta = 102.8998(11)^\circ$ , monoclinic,  $P2_1/c$ ,  $V = 5811.51(11) \text{ \AA}^3$ ,  $Z = 4$ ,  $R_1$  for 10758 [data intensity  $I > 2\sigma(I)$ ] unique reflections = 0.0368,  $wR_2$  (all 11964 unique reflections) = 0.0292. CCDC ref: 1055212.

**Reaction of 1-NH<sub>3</sub> with  $K[B(C_6F_5)_4]$ : Isolation of  $Sn\{B(NDippCH)_2\}_2(H)(NH_2)$ , **7**.** To a solution of 1-NH<sub>3</sub> (160 mg, 0.175 mmol) in benzene (2 mL) was added solid  $K[B(C_6F_5)_4]$  (162 mg, 0.225 mmol). Upon stirring at 20 °C the color of the mixture gradually changed from orange to light brown. After 1 h the mixture was filtered and the filtrate was evaporated in vacuo. A sample of the resulting crystalline material (21 mg) contained ca. 70%  $Sn\{B(NDippCH)_2\}_2(NH_2)(H)$ , together with unreacted 1-NH<sub>3</sub> (ca. 10%) and small quantities of **3**,  $HB(NDippCH)_2$  and  $H_2NB(NArCH)_2$  (as determined by <sup>1</sup>H NMR spectroscopy). Recrystallization from benzene/hexane (1:3) at 4 °C produced almost colorless blocks of benzene-solvated  $Sn\{B(NArCH)_2\}_2(NH_2)(H)$  (46 mg, 0.051 mmol, 29%), which lose crystallization solvent when taken from the mother solution and were unsuitable for X-ray diffraction. Single crystals were obtained by crystallization from methylcyclohexane at 4 °C (during crystallization solutions of  $Sn\{B(NArCH)_2\}_2(NH_2)(H)$  gradually turned dark brown or black resulting in low yields of pure crystals). <sup>1</sup>H NMR ( $C_6D_6$ ):  $\delta$  7.16 (4 H, m, *p*-H of Ar +  $C_6D_5H$ ), 7.05 (8 H, m, *m*-H of Ar), 6.16 (4 H, s, with <sup>119/117</sup>Sn satellites <sup>4</sup> $J(Sn-H) = 9.9$  Hz, NCH), 4.80 (br t, with <sup>119/117</sup>Sn satellites <sup>1</sup> $J(Sn-H) = 1365$  and 1430 Hz, SnH), 3.25 (4 H, septet, <sup>3</sup> $J = 6.87$  Hz,  $CHMe_2$ ), 3.00 (4 H, septet, <sup>3</sup> $J = 6.87$  Hz,  $CHMe_2$ ), 1.13 (12 H, d, <sup>3</sup> $J = 6.87$  Hz,  $CHMe_2$ ), 1.09 (36 H, overlapping doublets,  $CHMe_2$ ), -1.91 (2 H, br d, with <sup>119/117</sup>Sn satellites <sup>2</sup> $J(Sn-H) = 23$  Hz,  $SnNH_2$ ). Tin satellites for the SnH peak at  $\delta$  4.80 ppm were identified at  $\delta$  6.58 and 6.50 (the other pair of satellites overlaps with the septet at  $\delta$  3.00 ppm). <sup>13</sup>C{<sup>1</sup>H} NMR ( $C_6D_6$ ):  $\delta$  146.15 (*o*-C of Ar), 145.80 (*o*-C of Ar), 140.12 (*ipso*-C of Ar), 127.85 (*p*-CH of Ar), 124.00 (*m*-CH of Ar), 123.65 (*m*-CH of Ar), 122.89 (<sup>119/117</sup>Sn satellites <sup>3</sup> $J(Sn-C) = 36.0$  Hz, NCH), 28.80 ( $CHMe_2$ ), 28.66 ( $CHMe_2$ ), 25.78 ( $CHMe_2$ ), 25.55 ( $CHMe_2$ ), 24.04 ( $CHMe_2$ ), 23.34 ( $CHMe_2$ ). <sup>11</sup>B{<sup>1</sup>H} ( $C_6D_6$ ):  $\delta$  29.4. Crystallographic data (for **7**):  $C_{52}H_{75}B_2N_3Sn$ ,  $M_r = 910.51$ ,  $a = 21.2882(3) \text{ \AA}$ ,  $b = 12.5521(2) \text{ \AA}$ ,  $c = 19.6851(2) \text{ \AA}$ ,  $\beta = 98.1681(13)^\circ$ , monoclinic,  $P2_1/c$ ,  $V = 5206.7(1) \text{ \AA}^3$ ,  $Z = 4$ ,  $R_1$  for 10221 [data intensity  $I > 2\sigma(I)$ ] unique reflections = 0.0515,  $wR_2$  (all 10798 unique reflections) = 0.1147. CCDC ref: 1446877.

**$Sn\{B(NDippCH)_2\}_2(\mu-NH_2)_2$ , **8**.** A degassed solution of **2** (60 mg, 0.080 mmol) in  $C_6H_6$  (2 mL) was exposed to an atmosphere of ammonia and shaken by hand until the color changed from purple to light brown (~0.5 min). Volatiles were removed in vacuo, and the residue extracted into cyclohexane; the solution was concentrated and stored at 4 °C for 2 d yielding pale yellow block crystals of **8** (36 mg, 0.068 mmol of the monomer, 86%). Single crystals suitable for the X-ray diffraction were obtained from *n*-hexane, but the presence of residual solvent in the NMR sample prevented unambiguous assignment of the NH<sub>2</sub> group resonance; thus, cyclohexane was the solvent of choice for bulk preparation. Anal. found (calcd. for  $C_{26}H_{38}BN_2Sn$ ): C, 59.74 (59.81); H, 7.21 (7.34); N, 8.16 (8.05)%. <sup>1</sup>H NMR ( $C_6D_6$ ):  $\delta$  7.10 (2 H, dd, <sup>3</sup> $J = 6.2$  and 8.8 Hz, *p*-H of Ar), 7.04 (4 H, d, <sup>3</sup> $J = 7.7$  Hz, *m*-H of Ar), 6.40 (2 H, s, NCH), 3.44 (4 H, septet, <sup>3</sup> $J = 6.9$  Hz,  $CHMe_2$ ), 1.23 (12 H, d, <sup>3</sup> $J = 6.9$  Hz,  $CHMe_2$ ), 1.15 (12 H, d, <sup>3</sup> $J = 6.9$  Hz,  $CHMe_2$ ), 0.88 (2 H, br s,  $NH_2$ ). <sup>13</sup>C{<sup>1</sup>H} NMR ( $C_6D_6$ ):  $\delta$  146.41 (*o*-C of Ar), 140.45 (*ipso*-C of Ar), 127.58 (*p*-CH of Ar), 123.55 (*m*-CH of Ar), 121.50 (NCH), 28.64 ( $CHMe_2$ ), 26.11 ( $CHMe_2$ ), 23.79 ( $CHMe_2$ ). <sup>11</sup>B{<sup>1</sup>H} ( $C_6D_6$ ):  $\delta$  45.5. Crystallographic data (for **7**):  $C_{52}H_{75}B_2N_6Sn_2$ ,  $M_r = 1043.21$ ,  $a = 14.0818(3) \text{ \AA}$ ,  $b = 12.3113(2) \text{ \AA}$ ,  $c = 15.8745(2) \text{ \AA}$ ,  $\beta = 99.2666(15)^\circ$ , monoclinic,  $P2_1/c$ ,  $V = 2716.17(8) \text{ \AA}^3$ ,  $Z = 2$ ,  $R_1$  for 5398 [data intensity  $I > 2\sigma(I)$ ] unique reflections = 0.0223,  $wR_2$  (all 5596 unique reflections) = 0.0236. CCDC ref: 1055219.

**$KN\{B(NDippCH)_2\}_2(NH_2)_2$ , **9**.** Solid  $KN(SiMe_3)_2$  (55 mg, 0.276 mmol) was added to a solution of 1-NH<sub>3</sub> (252 mg, 0.276 mmol) in benzene (5 mL) at 20 °C. After stirring for 5 min, a deep yellow solution formed. Volatiles were removed in vacuo leading to the solution undergoing a color change to brown, and yellow crystalline material to precipitate. A small amount of the concentrated supernatant solution was sealed in a crystallization tube and stored

at 4 °C, producing yellow blocks suitable for X-ray crystallography. Washing of the crystalline product with cold hexane resulted in rapid darkening, therefore a small sample for spectroscopic characterization was prepared by crystallization from cyclohexane at 4 °C. The sample showed very broad resonances for Dipp substituents at 20 °C, which started to resolve at -10 °C; however, further cooling resulted in precipitation. <sup>1</sup>H NMR ( $C_6D_5CD_3$ , ref: internal  $SiMe_4$ ):  $\delta$  7.01–7.19 (12 H, br s, *p*- and *m*-H of Ar), 6.08 (4 H, s, NCH), 3.05 (8 H, v br s,  $CHMe_2$ ), 1.20 (48 H, br,  $CHMe_2$ ), -2.09 (2 H, br s,  $NH_2$ ). <sup>11</sup>B{<sup>1</sup>H} ( $C_6D_6$ ):  $\delta$  41.4. Attempts to obtain reliable <sup>13</sup>C NMR data for **9** were frustrated by its low solubility in compatible solvents. Crystallographic data (for **9**):  $C_{55}H_{77}B_2KN_5Sn$ ,  $M_r = 987.66$ ,  $a = 17.8585(1) \text{ \AA}$ ,  $b = 43.5512(2) \text{ \AA}$ ,  $c = 19.1937(1) \text{ \AA}$ ,  $\beta = 117.1098(3)^\circ$ , monoclinic,  $P2_1/a$ ,  $V = 13288.00(12) \text{ \AA}^3$ ,  $Z = 8$ ,  $R_1$  for 19623 [data intensity  $I > 2\sigma(I)$ ] unique reflections = 0.0576,  $wR_2$  (all 30117 unique reflections) = 0.1812. CCDC ref: 1446876.

**X-ray Crystallography.** X-ray diffraction data were collected at 150 K using either a Nonius Kappa CCD or Oxford Diffraction (Agilent) SuperNova A diffractometer.<sup>14a</sup> Structures were solved with SuperFlip,<sup>14b</sup> and refined by full-matrix least using CRYSTALS.<sup>14c</sup> Any disorder was modeled as per the CIF and hydrogen atoms were treated in the usual manner.<sup>14d</sup> Where the structure contained large solvent accessible voids comprising weak, diffuse electron density, the discrete Fourier transforms of the void regions were treated as contributions to the A and B parts of the calculated structure factors using PLATON/SQUEEZE integrated within the CRYSTALS software.<sup>14e</sup>

**Computational Details.** DFT calculations were performed using the Amsterdam Density Functional (ADF) Package Software 2012.<sup>15a-c</sup> Unrestricted calculations were performed using the Vosko–Wilk–Nusair local density approximation with exchange from Becke,<sup>15d</sup> and correlation corrections from Perdew (BP).<sup>15e</sup> Slater-type orbitals (STOs)<sup>15f</sup> were used for the triple- $\zeta$  basis set with an additional set of polarization functions (TZP). The large frozen core basis set approximation was applied with no molecular symmetry. The general numerical integration was 6. Relativistic effects were addressed using the scalar Zeroth Order Regular Approximation (ZORA).<sup>15g-i</sup> No significant imaginary frequencies were observed for the optimized geometry of the model complexes :MXY and [:MX(L)]<sup>+</sup>. See SI for the run files for frequency calculations, which contain coordinates for the optimized geometries of model complexes

## RESULTS AND DISCUSSION

**Computational Screening.** The singlet–triplet energy separation ( $\Delta E_{st}$ ) has previously been shown to be of key importance in determining activation barriers in the oxidative addition of E–H bonds at metallocene centers.<sup>5a,10</sup> With this in mind, we set out to probe (via DFT methods) the scope for tuning this gap in stannylene and related systems by variation in the peripheral substituents. These studies reveal that the incorporation of silyl, phosphido, or better still boryl substituents should lead to values for  $\Delta E_{st}$  of <15 kcal mol<sup>-1</sup> (Table 1), while the use of amido substituents, in particular, leads to significant stabilization of the singlet state ( $\Delta E_{st} > 21$  kcal mol<sup>-1</sup>). Such findings are in line with the notion that strongly  $\sigma$  electron-donating groups reduce the HOMO–LUMO gap through destabilization of the HOMO,<sup>16</sup> and the fact that ligands based around relatively electropositive atoms such as boron or silicon are among the strongest  $\sigma$ -donors currently available to the synthetic chemist.<sup>8</sup> Moreover, in contrast to the destabilization of the LUMO (and widening of the HOMO–LUMO gap) effected by  $\pi$ -donor substituents such as amido groups, it would also be expected that the moderate  $\pi$ -acceptor properties of the boryl ligand would, if anything, reduce the HOMO–LUMO gap, and hence also  $\Delta E_{st}$ .

The effect of net charge was also considered, given the isolobal relationship between formally anionic boryl and

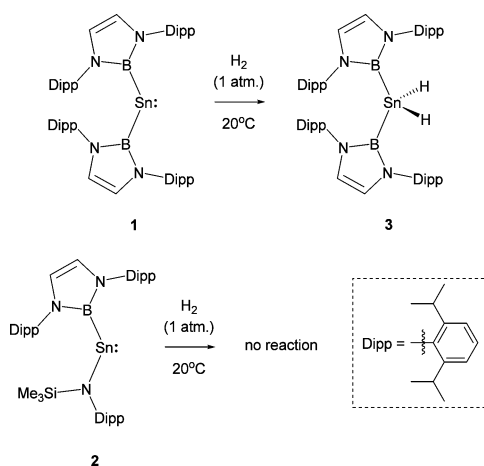
**Table 1.** DFT Calculated Singlet-Triplet Separation Energies,  $\Delta E_{st}$ , for Model Group 14 Metallylenes :MXY and [:MX(L)]<sup>+a</sup>

M	charge	X	Y	$\Delta E_{st}$ (kcal mol <sup>-1</sup> )
Sn	0	B(NMeCH) <sub>2</sub>	B(NMeCH) <sub>2</sub>	12.8
Sn	0	B(NMeCH) <sub>2</sub>	N(SiMe <sub>3</sub> )Me	23.5
Sn	0	B(NMeCH) <sub>2</sub>	PMe <sub>2</sub>	14.8
Sn	+1	B(NMeCH) <sub>2</sub>	C(NMeCH) <sub>2</sub>	22.3
Sn	0	Si(SiH <sub>3</sub> ) <sub>3</sub>	Si(SiH <sub>3</sub> ) <sub>3</sub>	14.5
Sn	0	Si(SiH <sub>3</sub> ) <sub>3</sub>	N(SiMe <sub>3</sub> )Me	24.5
Ge	0	B(NMeCH) <sub>2</sub>	B(NMeCH) <sub>2</sub>	10.5
Ge	0	B(NMeCH) <sub>2</sub>	N(SiMe <sub>3</sub> )Me	24.2
Si	0	B(NMeCH) <sub>2</sub>	B(NMeCH) <sub>2</sub>	7.8
Si	0	B(NMeCH) <sub>2</sub>	N(SiMe <sub>3</sub> )Me	21.4

<sup>a</sup>The corresponding value of  $\Delta E_{st}$  for the amido(silyl)silylene, Si{Si(SiMe<sub>3</sub>)<sub>3</sub>}{N(SiMe<sub>3</sub>)Dipp}, is calculated to be 24.8 kcal mol<sup>-1</sup>.<sup>11</sup>

charge-neutral N-heterocyclic carbene ligands, with the finding that preferential stabilization of the HOMO in the NHC-ligated cation leads to an enhanced magnitude of  $\Delta E_{st}$ . Bis(boryl)-germylene and -silylene systems were also evaluated (and shown to possess relatively low-lying triplet states), although in our hands such systems have yet to be accessed synthetically.<sup>17</sup> As such, boryl-stannylenes were considered to be a logical starting point for experimental studies, offering a workable compromise between accessibility and reactivity.

**Reactivity toward E–H Bonds (E = H, B, Si).** Diamido-stannylenes have previously been shown to be unreactive toward H<sub>2</sub>.<sup>18</sup> Given the predictions of enhanced reactivity associated with the incorporation of boryl substituents, the reactions of dihydrogen with (amido)borylstannylene **2** and homoleptic bis(boryl) stannylene **1** were therefore investigated (Scheme 1).<sup>9a</sup> Consistent with DFT predictions, we find that

**Scheme 1.** Contrasting Reactivity of Bis(boryl)- and (Amido)boryl Stannylene Complexes **1** and **2** toward H<sub>2</sub>

oxidative addition of H<sub>2</sub> at the tin center in **1** is facile, occurring steadily at room temperature to give the corresponding bis(boryl)tin(IV) dihydride **3**. By contrast, under analogous conditions **2** is unreactive toward dihydrogen, consistent with a significantly higher barrier to H–H bond activation.<sup>19,20</sup>

Characterization of **3** has been achieved by standard spectroscopic, analytical and crystallographic techniques; particularly diagnostic is the new NMR signal at  $\delta_H = 2.22$  ppm due to the SnH<sub>2</sub> unit, for which both <sup>117/119</sup>Sn satellites

can be resolved [<sup>1</sup>J(<sup>117</sup>Sn–<sup>1</sup>H) = 1277 Hz; <sup>1</sup>J(<sup>119</sup>Sn–<sup>1</sup>H) = 1337 Hz]. Consistently, the molecular structure determined by single crystal X-ray diffraction (Figure 1) features two tin-

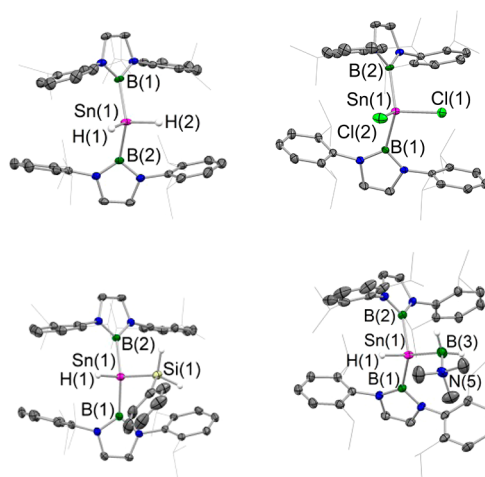


**Figure 1.** Molecular structures of **3**, Sn{B(NDippCH)<sub>2</sub>}<sub>2</sub>Cl<sub>2</sub>, **4b** and **5** as determined by X-ray crystallography. Most H atoms omitted and <sup>i</sup>Pr groups shown in wireframe format for clarity; thermal ellipsoids set at the 50% probability level. Key bond lengths (Å) and angles (°): (for **3**) Sn(1)–B 2.242(2), 2.246(2), Sn(1)–H 1.72(2), 1.72(2), B(1)–Sn(1)–B(2) 135.6(1); (for Sn{B(NDippCH)<sub>2</sub>}<sub>2</sub>Cl<sub>2</sub>) Sn(1)–B 2.250(3), 2.252(3), Sn(1)–Cl 2.353(1), 2.358(1), B(1)–Sn(1)–B(2) 136.3(1); (for **4b**) Sn(1)–B 2.248(5), 2.260(3), Sn(1)–H(1) 1.67(6), Sn(1)–Si(1) 2.593(1), B(1)–Sn(1)–B(2) 137.0(1); (for **5**) Sn(1)–B(1/2) 2.274(2), 2.284(2), Sn(1)–H(1) 1.68(2), Sn(1)–B(3) 2.272(3), B(3)–N(5) 1.621(4), B(1)–Sn(1)–B(2) 114.4(1).

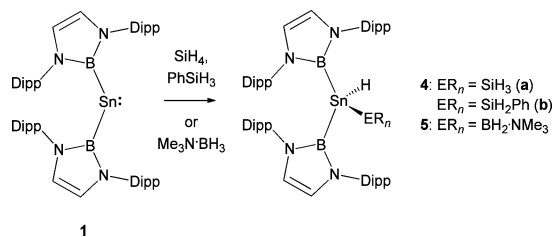
bound hydrogen atoms in the difference Fourier map, and a significantly widened B–Sn–B angle compared to bis(boryl)-stannylene precursor **1** [135.6(1) vs 118.8(3)°]. Similar phenomena have previously been observed in the oxidative addition of dihydrogen to lighter group 14 analogues [e.g., 109.7(1) and 120.1(1)°, respectively, for a (boryl)amidosilylene and the corresponding Si(IV) dihydride].<sup>9a,21</sup> In similar fashion, the B–Sn–B angle measured for Sn{B(NDippCH)<sub>2</sub>}<sub>2</sub>Cl<sub>2</sub> [which can be synthesized through the reaction of **1** with Ph<sub>3</sub>CCl or UCl<sub>4</sub> (SI)] shows a comparable widening [136.3(1)°]. Presumably, these observations reflect the shortening of the Sn–B bonds on oxidation from Sn<sup>II</sup> to Sn<sup>IV</sup> [e.g., 2.242(2), 2.246(2) Å for **3**, cf. 2.290(8) (mean) for **1**] and the consequent need to widen the B–Sn–B angle to minimize the repulsive interactions between the sterically very demanding boryl substituents.

While oxidative cleavage of dihydrogen at isolated carbene, silylene and germylene compounds has been reported previously,<sup>5,22–25</sup> to our knowledge the transformation of **1** to **3** represents the first example of simple oxidative addition of H<sub>2</sub> to a monometallic Sn<sup>II</sup> system to generate a Sn<sup>IV</sup> product. This process appears to be irreversible, and no hint of H–H or B–H elimination is observed from samples of **3** upon storing for several days at room temperature.

The presence of a relatively small singlet–triplet gap also facilitates the activation of a range of other E–H bonds by **1**, including hydridic systems such as B–H and Si–H bonds. Thus, silanes such as PhSiH<sub>3</sub> or SiH<sub>4</sub> itself, and boranes such as Me<sub>3</sub>N–BH<sub>3</sub>, undergo E–H oxidative addition to generate the corresponding silyl- or boryltin(IV) hydrides in moderate to good yield (**4a**, **4b**, **5**; Scheme 2).<sup>26,27</sup> To our knowledge, the

oxidative addition of Si–H and B–H bonds of this sort to give  $\text{Sn}^{\text{IV}}$  products has no precedent.<sup>26</sup>

**Scheme 2. Oxidative Addition of Hydridic E–H Bonds to 1 to Give Silyl and Boryl  $\text{Sn}^{\text{IV}}$  Species 4 and 5**



Here too, the appearance of the respective Sn–H resonance in the  $^1\text{H}$  NMR spectrum is diagnostic of the addition process. Thus, for example, in the case of **4a**, formed by the activation of  $\text{SiH}_4$ , the signal in question is a quartet [ $\delta_{\text{H}} = 1.66$  ppm,  $^3J(^1\text{H}-^1\text{H}) = 3.8$  Hz] with tin satellites [ $^1J(^{117}\text{Sn}-^1\text{H}) = 1223$  Hz;  $^1J(^{119}\text{Sn}-^1\text{H}) = 1281$  Hz], while the corresponding doublet  $\text{SiH}_3$  resonance shows coupling to both silicon and tin [ $\delta_{\text{H}} = 2.27$  ppm,  $^1J(^{29}\text{Si}-^1\text{H}) = 191.2$  Hz;  $^2J(^{117/119}\text{Sn}-^1\text{H}) = 39.9$  Hz]. In similar fashion, the analogous signals for the tin- and silicon-bound hydrogens in **4b** are a triplet [ $^3J(^1\text{H}-^1\text{H}) = 3.7$  Hz, with  $^{117/119}\text{Sn}$  satellites:  $^1J(^{117}\text{Sn}-^1\text{H}) = 1197$  Hz;  $^1J(^{119}\text{Sn}-^1\text{H}) = 1252$  Hz] and a lower field doublet [with  $^{29}\text{Si}$  and  $^{117/119}\text{Sn}$  satellites  $^1J(^{29}\text{Si}-^1\text{H}) = 190.3$  Hz;  $^2J(^{117/119}\text{Sn}-^1\text{H}) = 64.5$  Hz]. In the case of **5**,  $^1\text{H}-^1\text{H}$  couplings cannot be resolved, presumably due to broadening by the quadrupolar  $^{11}\text{B}$  nucleus of the  $-\text{BH}_2\text{-NMe}_3$  group; the presence of two distinct  $^{11}\text{B}$  environments is clearly signaled, however, by resonances at  $\delta_{\text{B}} = 31.9$  (for the three-coordinate boryl substituent) and  $-8.3$  ppm (for the four-coordinate base-stabilized boryl ligand). In addition, for both **4b** and **5**, structural authentication has proved possible by single crystal X-ray diffraction, which yields the heavy atom skeleton together with likely hydrogen atom positions from the difference Fourier map (Figure 1).

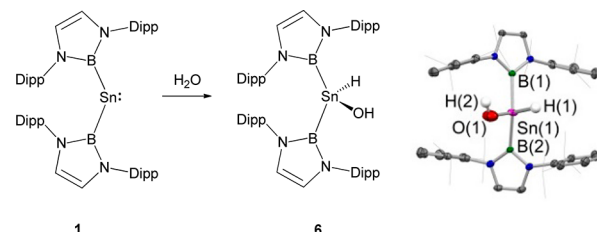
Interestingly, while the structure of **4b** features the wide B–Sn–B angle [ $137.0(1)^\circ$ ] characteristic of other  $\text{Sn}^{\text{IV}}$  systems (such as **3** and  $\text{Sn}\{\text{B}(\text{NDippCH}_2)_2\}_2\text{Cl}_2$ ), **5** possesses a much narrower angle at the metal center [ $114.4(1)^\circ$ ] and somewhat longer Sn–B(heterocycle) bonds [2.274(2), 2.284(2) Å cf. 2.242(2), 2.246(2) Å for **3**]. The bond to the  $-\text{BH}_2\text{-NMe}_3$  ligand is of similar length [2.272(3) Å] despite the higher coordination number at B(3) and is therefore clearly best described as a simple 2-center, 2-electron covalent bond (cf. 2.23 Å for the sum of the respective covalent radii).<sup>28</sup> We therefore attribute the narrower geometry of the bis(boryl)tin backbone in **5** to the higher steric demands of the relatively bulky  $-\text{BH}_2\text{-NMe}_3$  ligand (cf. H in **3**) in association with the short Sn–E distance (cf.  $\text{SiH}_2\text{Ph}$  in **4b**). An alternative description of **5** as a donor/acceptor adduct formed between a stannylene Lewis acid and  $\text{Me}_3\text{N}\cdot\text{BH}_3$  (acting as an essentially unactivated  $\sigma(\text{BH})$  donor) appears unlikely on the basis of the short Sn–B separation and the large Sn–H coupling constant (ca. 900 Hz).<sup>29</sup>

**Reactivity toward Protic E–H Bonds: Water.** The activation of protic E–H linkages by **1** has also been investigated, with both O–H and N–H bonds being shown to be amenable to oxidative addition. In contrast to compounds

**3–5**, however, the resulting  $\text{Sn}^{\text{IV}}$  products are prone to further reaction leading to B–E reductive elimination ( $\text{E} = \text{O}, \text{N}$ ).

In the case of water, the hydroxytin(IV) hydride  $\text{Sn}\{\text{B}(\text{NDippCH}_2)_2\}_2(\text{H})(\text{OH})$ , **6**, resulting from the oxidative addition of one O–H bond can be isolated in very good yield (85%, Scheme 3) and characterized by multinuclear NMR, X-

**Scheme 3. Oxidative Addition of the O–H Bond in Water to 1 to Give Hydroxy  $\text{Sn}^{\text{IV}}$  Hydride **6**<sup>a</sup>**



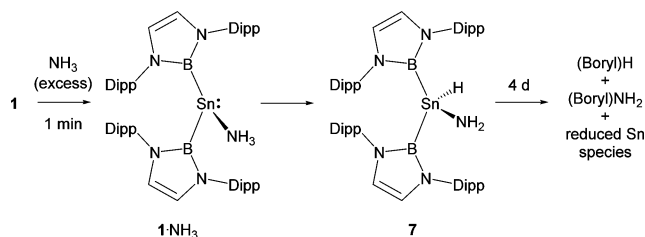
<sup>a</sup>Molecular structure of **6** as determined by X-ray crystallography. Most H atoms omitted and  $^i\text{Pr}$  groups shown in wireframe format for clarity; thermal ellipsoids set at the 50% probability level. Key bond lengths (Å) and angles ( $^\circ$ ): Sn(1)–B(1/2) 2.251(2), 2.259(2), Sn(1)–H(1) 1.76, Sn(1)–O(1) 1.977(2), B(1)–Sn(1)–B(2) 138.7(1).

ray crystallography and elemental microanalysis. As in the cases of H–H, B–H and Si–H oxidative addition products, the resulting Sn–H linkage is characterized in solution by large satellite couplings to  $^{117/119}\text{Sn}$  [ $^1J(^{117}\text{Sn}-^1\text{H}) = 1385$  Hz;  $^1J(^{119}\text{Sn}-^1\text{H}) = 1456$  Hz], while the (sharper) SnOH resonance can be resolved into a doublet [ $^3J(^1\text{H}-^1\text{H}) = 1.4$  Hz] with longer range couplings to tin [ $^2J(^{117/119}\text{Sn}-^1\text{H}) = 24.6$  Hz].

While the oxidative addition of water to a single main group metal center is very rare, precedent does exist for  $\text{Sn}^{\text{II}}$ , with Pörschke and co-workers reporting the synthesis of  $\text{Sn}\{\text{CH}(\text{SiMe}_3)_2\}_2(\text{H})(\text{OH})$  from the corresponding stannylene as long ago as 1998.<sup>6a,d</sup> The molecular structures of these two systems are similar, featuring Sn–O distances of 1.977(2) (for **6**; Scheme 3) and 1.984(1) Å; however, while  $\text{Sn}\{\text{CH}(\text{SiMe}_3)_2\}_2(\text{H})(\text{OH})$  aggregates into centrosymmetric dimers via pairs of  $\text{OH}\cdots\text{O}$  hydrogen bonds, **6** is mononuclear in the solid state, presumably reflecting the greater steric bulk of the ancillary boryl ligands. The wide B–Sn–B angle measured for **6** [ $138.7(1)^\circ$ ] is consistent with those reported for **3**, **4b** and  $\text{Sn}\{\text{B}(\text{NDippCH}_2)_2\}_2\text{Cl}_2$ .

In contrast to the  $\text{Sn}^{\text{IV}}$  compounds formed by the oxidative addition of hydridic E–H bonds, however, **6** undergoes further reaction at elevated temperatures. Thus, refluxing in hexane leads to the formation of equimolar amounts of  $\text{HB}(\text{NDippCH}_2)_2$  and  $\text{HOB}(\text{NDippCH}_2)_2$  together with tin metal. This chemistry is thought to be initiated by the reductive elimination of the strong B–O bond from **6** and appears closely related to the onward reactivity of the corresponding ammonia activation product (vide infra).

**Reactivity toward Protic E–H Bonds: Ammonia.** The oxidative addition of N–H bonds in ammonia represents a high profile challenge in synthetic chemistry in part because of the dearth of transition metal systems capable of effecting such a transformation,<sup>30</sup> and the relevance of N–H activation to a number of potentially important industrial processes.<sup>31</sup> Thus, the reactivity of **1** toward  $\text{NH}_3$  has also been explored (Scheme 4).<sup>32</sup>

**Scheme 4. Reaction of 1 with Ammonia: Coordination, N–H Activation and Subsequent B–N/B–H Reductive Elimination**


Addition of excess ammonia to a benzene solution of **1** rapidly yields a compound of composition  $\mathbf{1}\cdot\text{NH}_3$ , which is characterized by a marked downfield shift in the  $\text{NH}_3$  resonance, from  $\delta_{\text{H}} = -0.17$  (free  $\text{NH}_3$ ) to 0.32 ppm (isolated  $\mathbf{1}\cdot\text{NH}_3$ ; samples containing excess  $\text{NH}_3$  show intermediate shift), and by slow onward reaction in  $\text{C}_6\text{D}_6$  solution. Monitoring of the latter by in situ NMR measurements leads to two key observations: (i) the formation of an intermediate species characterized by mutually coupled ( $^1\text{H}$ – $^1\text{H}$  COSY spectrum) broad resonances with relative intensities of 1:2, which, although labile, persists for up to 4 days under certain conditions, and (ii) the formation of the final products, namely a  $\sim 1:1$  mixture of  $\text{H}_2\text{NB}(\text{NDippCH})_2$  and  $\text{HB}(\text{NDippCH})_2$ , together with reduced tin species. The amidoborane  $\text{H}_2\text{NB}(\text{NDippCH})_2$  can be synthesized independently from  $\text{KNH}_2$  and  $\text{BrB}(\text{NDippCH})_2$  for proof of composition (see SI).<sup>9c</sup> In addition, the metal-containing product is shown to be primarily elemental tin, although we were also able (reproducibly) to isolate very small quantities of two tin clusters, identified as *nido*- $\text{Sn}_{11}\{\text{B}(\text{NDippCH})_2\}_4$  and *nido*- $\text{Sn}_{10}\{\text{B}(\text{NDippCH})_2\}_4$  on the basis of X-ray crystallographic studies (see SI), which also speak to the reductive nature of B–N/B–H bond formation.

Our interpretation of these data in terms of a likely mechanistic pathway involves initial formation of a simple donor/acceptor adduct  $\mathbf{1}\cdot\text{NH}_3$  featuring the stannylene **1** acting as a Lewis acid. Indeed, this intermediate species can be isolated by removal of volatiles in vacuo at short reaction times and characterized by multinuclear NMR spectroscopy and X-ray crystallography (Scheme 4 and Figure 2).  $\mathbf{1}\cdot\text{NH}_3$  is labile toward further onward reaction and our initial attempts to obtain single crystals were unsuccessful. With this in mind we also synthesized the related *tert*-butylamine adduct  $\mathbf{1}\cdot\text{NH}_2^t\text{Bu}$  through the corresponding reaction of **1** with  $^t\text{BuNH}_2$ , and additionally characterized this system by standard spectroscopic and crystallographic techniques (Figure 2).

From a structural perspective, both  $\mathbf{1}\cdot\text{NH}_3$  and  $\mathbf{1}\cdot\text{NH}_2^t\text{Bu}$  can be shown to feature the N-donor coordinated essentially perpendicular to the plane of a  $\text{SnB}_2$  unit, which is itself largely unperturbed from that found in the free stannylene [e.g., for  $\mathbf{1}\cdot\text{NH}_3$ :  $\angle\text{N}(2)\text{–Sn}(1)\text{–B}(3/33) = 92.4(1), 94.6(1)^\circ$ ;  $\angle\text{B}(3)\text{–Sn}(1)\text{–B}(33) = 119.3(1)^\circ$ ]. Such data are consistent with descriptions of these systems as Lewis acid/base adducts formed by interaction of the amine lone pair with the formally vacant  $p\pi$  orbital at tin. The Sn–N bond lengths for both systems [2.355(3) and 2.350(2) Å] are in keeping with other three-coordinate N-donor stannylene adducts [e.g., 2.345(6) Å for an intramolecular pyridine stabilized (dialkyl)stannylene].<sup>33</sup>

The behavior of  $\mathbf{1}\cdot\text{NH}_3$  in solution is found to be strongly dependent on the concentration of free ammonia present. Thus, while isolated single crystalline samples react slowly

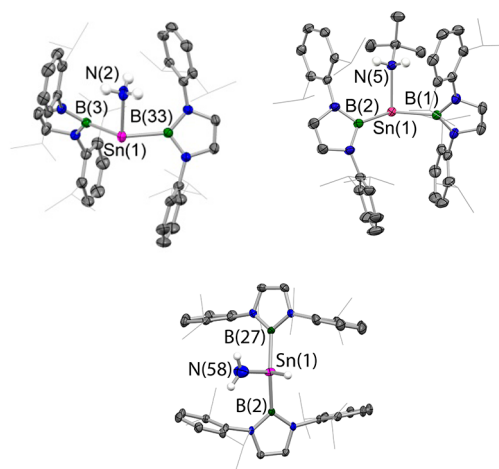


**Figure 2.** Molecular structures of  $\mathbf{1}\cdot\text{NH}_3$  (upper left),  $\mathbf{1}\cdot\text{NH}_2^t\text{Bu}$  (upper right) and **7** as determined by X-ray crystallography. Most hydrogen atoms omitted, and  $^i\text{Pr}$  groups shown in wireframe format for clarity; thermal ellipsoids set at the 50% probability level. Key bond lengths (Å) and angles ( $^\circ$ ): (for  $\mathbf{1}\cdot\text{NH}_3$ ) Sn(1)–B 2.311(3), 2.306(3), Sn(1)–N(2) 2.355(3), B(3)–Sn(1)–B(33) 119.3(1), N(2)–Sn(1)–B 92.4(1), 94.6(1); (for  $\mathbf{1}\cdot\text{NH}_2^t\text{Bu}$ ) Sn(1)–B 2.323(2), 2.338(2), Sn(1)–N(5) 2.350(2), B(1)–Sn(1)–B(2) 118.3(1), N(5)–Sn(1)–B 90.3(1), 95.4(1); (for **7**): Sn(1)–B 2.251(4), 2.259(3), Sn(1)–N(58) 1.969(5), B(2)–Sn(1)–B(27) 138.2(1).

(<50% conversion to a mixture of **7**,  $\text{H}_2\text{NB}(\text{NDippCH})_2$ ,  $\text{HB}(\text{NDippCH})_2$  over 44 h at 20  $^\circ\text{C}$ ), the presence of a 2-fold excess of ammonia leads to more rapid onward reaction with little of the adduct remaining after 21 h under otherwise analogous conditions. The spectroscopic properties of  $\mathbf{1}\cdot\text{NH}_3$  are also dependent on the presence of additional free ammonia in solution. Thus, isolated crystalline samples of the adduct display two broad resonances for the Dipp methine protons at 20  $^\circ\text{C}$ , which sharpen on cooling below 0  $^\circ\text{C}$ , and which form one broad signal at 50  $^\circ\text{C}$ . This observation is ascribed to slow rotation about the Sn–B bonds in  $\mathbf{1}\cdot\text{NH}_3$  on the NMR time scale, which renders inequivalent the two Dipp groups associated with each boryl ligand. Conceivably, the fluxional process occurring in the higher temperature regime may involve either rotation about the Sn–B bonds, or loss of the  $\text{NH}_3$  ligand/recoordination at either of the two faces of the  $\text{SnB}_2$  unit. With the latter mechanism in mind, it is notable that exchange is more facile in the presence of added ammonia (with a sharp septet being observed for the Dipp methine protons at 20  $^\circ\text{C}$ ).

Following coordination of  $\text{NH}_3$ , N–H bond cleavage then occurs, generating the amidotin(IV) hydride  $\text{Sn}\{\text{B}(\text{NDippCH})_2\}_2(\text{H})(\text{NH}_2)$  (**7**), analogous to the (hydroxy)tin hydride **6** isolated from the reaction of **1** with water.<sup>34</sup> The formation of isolable phosphidotin(IV) hydrides by the oxidative addition of P–H bonds to diaryl stannylenes has also been reported recently.<sup>14</sup>

Spectroscopically, such an (amido)hydride species is consistent with the pattern of  $^1\text{H}$  NMR resonances observed in situ [ $\delta_{\text{H}} = 4.80$  (1H, SnH),  $-1.90$  ppm (2H,  $\text{SnNH}_2$ )]. These can be compared to shifts of  $\delta_{\text{H}} = 6.13$  (1H, SnH),  $-2.09$  ppm (1H, SnOH) for **6**, and  $\delta_{\text{H}} = 5.22$  (1H, SiH), 0.99 ppm (2H,  $\text{SiNH}_2$ ) for the thermally stable (and crystallographically characterized) silicon (amido)hydride  $\text{Si}\{\text{Si}(\text{SiMe}_3)_3\}\text{N}(\text{SiMe}_3)\text{Dipp}\{\text{H}\}(\text{NH}_2)$  synthesized via the

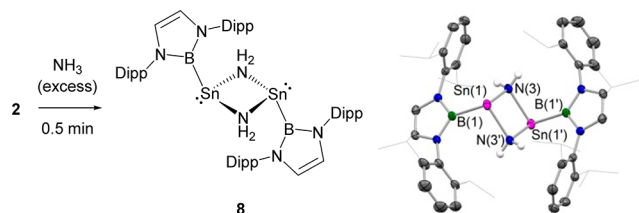
reaction of the acyclic silylene  $\text{Si}\{\text{Si}(\text{Me}_3)_3\}\{\text{N}(\text{SiMe}_3)\text{Dipp}\}$  with ammonia (SI).

The apparently comparable rates of formation of **7** (from  $1\cdot\text{NH}_3$ ), and its onward conversion (to  $\text{H}_2\text{NB}(\text{NDippCH})_2$  and  $\text{HB}(\text{NDippCH})_2$ ) render it impossible to obtain significant amounts of this compound via this route. More rapid conversion of  $1\cdot\text{NH}_3$  into **7** can be achieved by employing an alternative acid/base synthetic methodology (vide infra). Single crystals of **7** suitable for X-ray crystallography could be obtained via the Lewis acid ( $\text{K}[\text{B}(\text{C}_6\text{F}_5)_4]$ ) catalyzed isomerization of  $1\cdot\text{NH}_3$  (Figure 2). The crystals of **7** so obtained are isomorphous with those of **6**, but can be shown unequivocally to contain the (amido)tin hydride on the basis of multinuclear NMR measurements made on single crystalline samples redissolved in  $\text{C}_6\text{D}_6$ . Moreover, the  $^1\text{H}$  NMR signals associated with the  $\text{SnH}$  and  $\text{SnNH}_2$  units are found at chemical shifts indistinguishable from those measured in situ for the intermediate species in the  $1/\text{NH}_3$  reaction.

The onward lability of **7** is in line with (i) previous literature reports describing facile coupling between adjacent metal-bound borane moieties and electron-rich coligands;<sup>35</sup> and (ii) the observation that isolated (hydroxy)hydride **6** also undergoes elimination of equimolar quantities of hydro- and hydroxyborane (albeit more slowly). In the case of  $\text{Sn}\{\text{B}(\text{NDippCH})_2\}_2(\text{H})(\text{NH}_2)$ , reductive elimination of the strong B–N bond formed by coupling of  $\pi$ -donor amido and  $\pi$ -acceptor boryl components would represent a thermodynamic driving force, and account for the formation of  $\text{H}_2\text{NB}(\text{NDippCH})_2$ . Subsequent B–H extrusion then generates the observed hydroborane  $\text{HB}(\text{NDippCH})_2$  and a source of  $\text{Sn}^0$ , which is either precipitated as the metal itself, or trapped by unreacted  $1\cdot\text{NH}_3$  to generate the observed small quantities of  $\text{Sn}_{10}$  and  $\text{Sn}_{11}$ -clusters. We favor this ordering of the reductive elimination steps (i.e., B–N formation preceding B–H) on the basis that the  $\text{Sn}^{\text{II}}$  amide  $[\text{Sn}\{\text{B}(\text{NDippCH})_2\}_2(\text{NH}_2)]_2$  can be shown to be stable with respect to B–N elimination, and thus not a viable intermediate under the conditions employed.

Independent synthesis of a complex of composition  $[\text{Sn}\{\text{B}(\text{NDippCH})_2\}_2(\text{NH}_2)]$  can be achieved by the reaction of amido(boryl)stannylene **2** with ammonia. In this case conversion proceeds rapidly (<1 min) via a formal acid/base reaction. Thus, protonolysis generates the free aniline  $\text{HN}(\text{SiMe}_3)\text{Dipp}$  and the dinuclear primary amidostannylene  $[\text{Sn}\{\text{B}(\text{NDippCH})_2\}_2(\mu\text{-NH}_2)]_2$  (**8**; Scheme 5), the identity of which has been confirmed crystallographically. Such chemistry, leading as it does to the isolation of a  $\text{Sn}^{\text{II}}$  amide, mirrors the

**Scheme 5. Protonolysis of Amidostannylene 2 by Ammonia<sup>a</sup>**

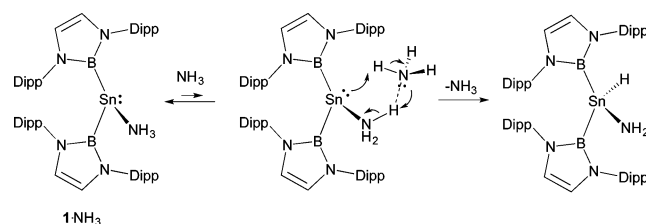


<sup>a</sup>Molecular structure of **8** as determined by X-ray crystallography. Most hydrogen atoms omitted, and 'Pr groups shown in wireframe format for clarity; thermal ellipsoids set at the 50% probability level. Key bond lengths (Å) and angles (°):  $\text{Sn}(1)\text{--B}(1)$  2.309(2),  $\text{Sn}(1)\text{--N}(3)$  2.215(1),  $\text{Sn}(1)\text{--N}(3')$  2.227(1),  $\text{B}(1)\text{--Sn}(1)\text{--N}(3)$  90.4(1),  $\text{B}(1)\text{--Sn}(1)\text{--N}(1')$  92.9(1),  $\text{N}(1)\text{--Sn}(1)\text{--N}(1')$  80.7(1).

reactivity toward ammonia reported by Power and co-workers for diarylstannylene systems.<sup>5</sup> Moreover, in line with the mechanistic proposals outlined above, in our hands **8** is found to be essentially inert to B–N reductive elimination.

Classical mechanisms of concerted E–H bond activation at a single transition metal center involve donation of electron density from the E–H  $\sigma$  bonding orbital and back-bonding into the corresponding  $\sigma^*$  orbital.<sup>1</sup> The activation of  $\text{H}_2$  by acyclic silylenes is also thought to involve initial interaction of the H–H  $\sigma$ -bonding MO with the  $p\pi$  orbital of the electrophilic silicon center,<sup>9a</sup> while alternative mechanisms exploiting the strongly nucleophilic carbon-centered lone pair have been advanced for E–H activation by related carbene compounds.<sup>24</sup> With regard to the activation of ammonia by metallylene systems, an alternative mechanistic pathway which has been proposed computationally,<sup>5b,34,36</sup> involves a second molecule of  $\text{NH}_3$  acting as a proton shuttle, in effect transferring  $\text{H}^+$  from a coordinated ammonia molecule to the Group 14 center. Thus, computational studies from Power and Nagase, Pörschke and Sicilia, for example, all propose that such a mechanism ought to be viable for the activation of ammonia (and indeed water) by low valent Group 14 metal centers.<sup>5b,6a,d,34,36</sup> In the case of ammonia activation by **1**, we wondered whether the significantly increased rate of onward reaction of  $1\cdot\text{NH}_3$  in the presence of excess ammonia might be explained on the basis of a similar mechanism (Scheme 6). Therefore, with a

**Scheme 6. Potential Proton Shuttling Mechanism for N–H activation in  $1\cdot\text{NH}_3$  Involving a Second Molecule of Ammonia**



view to probing the plausibility of such deprotonation at N/protonation at Sn acid/base chemistry we set out to isolate the conjugate base of  $1\cdot\text{NH}_3$ , and examine its behavior in the presence of ammonium salts (i.e., sources of  $\text{H}^+$ ).

In the event, the reaction of  $\text{K}[\text{N}(\text{SiMe}_3)_2]$  with  $1\cdot\text{NH}_3$  does indeed lead to deprotonation of the tin-bound ammonia molecule and to the formation of the potassium salt of the  $[\text{Sn}\{\text{B}(\text{NDippCH})_2\}_2(\text{NH}_2)]^-$  anion. Confirmation of the nature of the product could be obtained crystallographically, with the structure shown to feature centrosymmetric dimers in the solid state (**9**; Figure 3).

Deprotonation is accompanied by a marked shortening of the Sn–N distance [2.088(8) Å cf. 2.355(2) Å for  $1\cdot\text{NH}_3$ ], and  $\text{Sn}(1)$  is also engaged in a contact with the potassium cation [ $d(\text{Sn}\cdots\text{K}) = 3.745(2)$  Å] which is well within the sum of the respective van der Waals radii. This observation is consistent with the presence of significant electron density at the  $\text{Sn}^{\text{II}}$  center, and accordingly, reaction of **9** with the dialkylanilinium salt  $[\text{HNMe}_2\text{Ph}][\text{B}(\text{C}_6\text{F}_5)_4]$ , in  $\text{C}_6\text{D}_6$  at 20 °C generates a ~2:1 mixture of  $\text{Sn}\{\text{B}(\text{NDippCH})_2\}_2(\text{H})(\text{NH}_2)$  (**7**) and  $1\cdot\text{NH}_3$ . This mixture presumably reflects the kinetics of protonation at Sn and N, since the mixture transforms to yield solely the thermodynamic product (**7**) after 6 h at 20 °C. As such, the notion of N–H oxidative addition occurring via coordination of



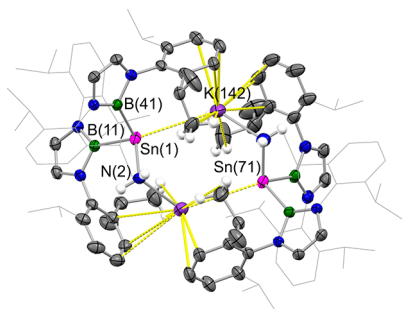


**Figure 3.** Molecular structure of dimeric **9** as determined by X-ray crystallography. Most hydrogen atoms omitted, and selected carbon atoms shown in wireframe format for clarity; thermal ellipsoids set at the 50% probability level. Key bond lengths (Å) and angles (°): Sn(1)–B 2.302(4), 2.314(5), Sn(1)–N(2) 2.088(8), Sn(1)⋯K(142) 3.745(2), B(11)–Sn(1)–B(41) 102.7(2), N(2)–Sn(1)–B 102.8(2), 104.3(2).

NH<sub>3</sub>, followed by N-donor mediated proton transfer, can be shown to have some experimental validity. Finally, we note that the transformation of **1**·NH<sub>3</sub> into **7** can also be brought about, cleanly and in catalytic fashion by employing ca. 10 mol % of the solvent-free potassium borate K[B(C<sub>6</sub>F<sub>5</sub>)<sub>4</sub>]. Mechanistically, this process is proposed to occur via Lewis acid sequestration of NH<sub>3</sub> from **1**·NH<sub>3</sub> by K<sup>+</sup>, resulting in the presence in solution of a small quantity of species of the type [K(NH<sub>3</sub>)<sub>x</sub>]<sup>+</sup>. The enhanced acidity of the N–H protons in such species presumably then facilitates isomerization via protonation at tin. Consistent with this hypothesis, the direct conversion of **1**·NH<sub>3</sub> to **7** can also be brought about by the addition of a catalytic amount (ca. 5 mol %) of [HNMe<sub>2</sub>Ph][B(C<sub>6</sub>F<sub>5</sub>)<sub>4</sub>] (see SI).

## CONCLUSIONS

In conclusion, we have demonstrated that a bis(boryl) ancillary ligand set can facilitate the oxidative addition of a range of E–H bonds at Sn<sup>II</sup> from both a thermodynamic and a kinetic viewpoint. Moreover, in the case of O–H and N–H bonds, the formation via oxidative addition of a tin-bound  $\pi$ -donor ligand offers a facile route to E–B bond formation (E = O, N) and re-reduction of the tin center. Thus, a single-center redox-based bond modification process is unequivocally established for a main group metal. From a mechanistic viewpoint, a two-step coordination/proton transfer process for N–H activation is shown to be viable through the isolation of intermediate species of the types Sn(boryl)<sub>2</sub>·NH<sub>3</sub> and [Sn(boryl)<sub>2</sub>(NH<sub>2</sub>)]<sup>−</sup>, and protonation of the latter to give Sn(boryl)<sub>2</sub>(H)(NH<sub>2</sub>).

## ASSOCIATED CONTENT

### Supporting Information

The Supporting Information is available free of charge on the ACS Publications website at DOI: 10.1021/jacs.6b00710.

Additional synthetic/characterizing data, copies of NMR spectra for new compounds, and complete details of DFT calculations (including run files). (PDF)

Crystal data. (CIF)

## AUTHOR INFORMATION

### Corresponding Author

\*simon.aldridge@chem.ox.ac.uk

## Notes

The authors declare no competing financial interest.

## ACKNOWLEDGMENTS

We acknowledge the NMSF, Swansea University. We thank the Leverhulme Trust (F/08 699/E), the OUP John Fell Fund, the ARC, the EU (Marie Curie grant PIEF-GA-2013–626441), NSERC and the EPSRC (EP/L025000/1 and EP/K014714/1) for funding various aspects of this work.

## REFERENCES

- (1) See, for example: Hartwig, J. F. In *Organotransition Metal Chemistry: From Bonding to Catalysis*; University Science Books: Sausalito, CA, 2010.
- (2) For discussions of potential redox-based bond modification processes based on phosphorus, see: (a) Dunn, N. L.; Ha, M.; Radosevich, A. T. *J. Am. Chem. Soc.* **2012**, *134*, 11330–11333. (b) Zeng, G.; Maeda, S.; Taketsugu, T.; Sakaki, S. *Angew. Chem., Int. Ed.* **2014**, *53*, 4633–4637. (c) Cui, J.; Li, Y.; Ganguly, R.; Inthirarajah, A.; Hirao, H.; Kinjo, R. *J. Am. Chem. Soc.* **2014**, *136*, 16764–16767. (d) Zhao, W.; McCarthy, S. M.; Lai, T. Y.; Yennawar, H. P.; Radosevich, A. T. *J. Am. Chem. Soc.* **2014**, *136*, 17634–17644. (e) Robinson, T. P.; De Rosa, D. M.; Aldridge, S.; Goicoechea, J. M. *Angew. Chem., Int. Ed.* **2015**, *54*, 13758–13763. For a more broad-ranging comparative discussion of main group elements and transition metals, see: (f) Power, P. P. *Nature* **2010**, *463*, 171–177.
- (3) (a) Martin, D.; Soleilhavoup, M.; Bertrand, G. *Chem. Sci.* **2011**, *2*, 389–399. See also: (b) Mizuhata, Y.; Sasamori, T.; Tokitoh, N. *Chem. Rev.* **2009**, *109*, 3479–3511. (c) Yao, S.; Xiong, Y.; Driess, M. *Organometallics* **2011**, *30*, 1748–1767.
- (4) Reversible E–H bond activation at a carbene: (a) Moerdyk, J. P.; Blake, G. A.; Chase, D. T.; Bielawski, C. W. *J. Am. Chem. Soc.* **2013**, *135*, 18798–18801. Reversible (formally oxidative) coordination of ethylene at Group 14 centers: (b) Peng, Y.; Ellis, B. D.; Wang, X.; Fettingter, J. C.; Power, P. P. *Science* **2009**, *325*, 1668–1670. (c) Lips, F.; Fettingter, J. C.; Mansikkamäki, A.; Tuononen, H. M.; Power, P. P. *J. Am. Chem. Soc.* **2014**, *136*, 634–637.
- (5) (a) Peng, Y.; Ellis, B. D.; Wang, X.; Power, P. P. *J. Am. Chem. Soc.* **2008**, *130*, 12268–12269. (b) Peng, Y.; Guo, J.-D.; Ellis, B. D.; Zhu, Z.; Fettingter, J. C.; Power, P. P. *J. Am. Chem. Soc.* **2009**, *131*, 16272–16282. See also: (c) Inomata, K.; Watanabe, T.; Miyazaki, Y.; Tobita, H. *J. Am. Chem. Soc.* **2015**, *137*, 11935–11937.
- (6) Formal E–H bond oxidative addition at Sn<sup>II</sup>: (a) Schager, F.; Goddard, R.; Seevogel, K.; Pörschke, K.-R. *Organometallics* **1998**, *17*, 1546–1551. (b) Brown, Z. D.; Erickson, J. D.; Fettingter, J. C.; Power, P. P. *Organometallics* **2013**, *32*, 617–622. (c) Dube, J. W.; Brown, Z. D.; Caputo, C. A.; Power, P. P.; Ragona, P. J. *Chem. Commun.* **2014**, *50*, 1944–1946. (d) Erickson, J. D.; Vasko, P.; Riparetti, R. D.; Fettingter, J. C.; Tuononen, H. M.; Power, P. P. *Organometallics* **2015**, *34*, 5785–5791. For an example of H<sub>2</sub> activation at a distannyne, RSnSnR, see: (e) Peng, Y.; Brynda, M.; Ellis, B. D.; Fettingter, J. C.; Rivard, E.; Power, P. P. *Chem. Commun.* **2008**, 6042–6044. (f) Power, P. P. *Acc. Chem. Res.* **2011**, *44*, 627–637. See also: (g) Vasko, P.; Wang, S.; Tuononen, H. M.; Power, P. P. *Angew. Chem., Int. Ed.* **2015**, *54*, 3802–3805.
- (7) For a recent example of the reductive elimination of H<sub>2</sub> from Sn<sup>IV</sup>, see: Sindlinger, C. P.; Stasch, A.; Bettinger, H. F.; Wesemann, L. *Chem. Sci.* **2015**, *6*, 4737–4751.
- (8) (a) Zhu, J.; Lin, Z.; Marder, T. B. *Inorg. Chem.* **2005**, *44*, 9384–9390. (b) Braunschweig, H.; Dewhurst, R. D.; Schneider, A. *Chem. Rev.* **2010**, *110*, 3924–3957.
- (9) Syntheses of boryltin systems: (a) Protchenko, A. V.; Birjukumar, K. H.; Dange, D.; Schwarz, A. D.; Vidovic, D.; Jones, C.; Kaltsoyannis, N.; Mountford, P.; Aldridge, S. *J. Am. Chem. Soc.* **2012**, *134*, 6500–6503. (b) Protchenko, A. V.; Dange, D.; Schwarz, A. D.; Tang, C. Y.; Phillips, N.; Mountford, P.; Jones, C.; Aldridge, S. *Chem. Commun.* **2014**, *50*, 3841–3844. For a related (boryl)amidotin compound, see:

- (c) Hadlington, T. J.; Abdalla, J. A. B.; Tirfoin, R.; Aldridge, S.; Jones, C. *Chem. Commun.* **2016**, 52, 1717–1720.
- (10) Wang, Y.; Ma, J. *J. Organomet. Chem.* **2009**, 694, 2567–2575.
- (11) Protchenko, A. V.; Schwarz, A. D.; Blake, M. P.; Jones, C.; Kaltsoyannis, N.; Mountford, P.; Aldridge, S. *Angew. Chem., Int. Ed.* **2013**, 52, 568–571.
- (12) Finholt, A. E.; Bond, A. C., Jr.; Wilzbach, K. E.; Schlesinger, H. I. *J. Am. Chem. Soc.* **1947**, 69, 2692–2696.
- (13) Segawa, Y.; Yamashita, M.; Nozaki, K. *Science* **2006**, 314, 113–115.
- (14) (a) Cosier, J.; Glazer, A. M. *J. Appl. Crystallogr.* **1986**, 19, 105–107. (b) Palatinus, L.; Chapuis, G. *J. Appl. Crystallogr.* **2007**, 40, 786–790. (c) Betteridge, P. W.; Carruthers, J. R.; Cooper, R. I.; Prout, K.; Watkin, D. J. *J. Appl. Crystallogr.* **2003**, 36, 1487. (d) Cooper, R. I.; Thompson, A. L.; Watkin, D. J. *J. Appl. Crystallogr.* **2010**, 43, 1100–1107. (e) Spek, A. L. *J. Appl. Crystallogr.* **2003**, 36, 7–13. (f) van der Sluis, P.; Spek, A. L. *Acta Crystallogr., Sect. A: Found. Crystallogr.* **1990**, A46, 194–201.
- (15) (a) te Velde, G.; Bickelhaupt, F. M.; Baerends, E. J.; Fonseca Guerra, C.; van Gisbergen, S. J. A.; Snijders, J. G.; Ziegler, T. *J. Comput. Chem.* **2001**, 22, 931–967. (b) Fonseca Guerra, C.; Snijders, J. G.; te Velde, G.; Baerends, E. J. *Theor. Chem. Acc.* **1998**, 99, 391–403. (c) ADF2012, SCM, Theoretical Chemistry, Vrije Universiteit: Amsterdam, The Netherlands; <http://www.scm.com>. (d) Becke, A. D. *Phys. Rev. A: At., Mol., Opt. Phys.* **1988**, 38, 3098–3100. (e) Perdew, J. P. *Phys. Rev. B: Condens. Matter Mater. Phys.* **1986**, 33, 8822–8824. (f) Snijders, J. G.; Vernooijs, P.; Baerends, E. J. *At. Data Nucl. Data Tables* **1982**, 26, 483–509. (g) van Lenthe, E.; Baerends, E. J.; Snijders, J. G. *J. Chem. Phys.* **1993**, 99, 4597–4610. (h) van Lenthe, E.; Baerends, E. J.; Snijders, J. G. *J. Chem. Phys.* **1994**, 101, 9783–9792. (i) van Lenthe, E.; Ehlers, A.; Baerends, E. J. *J. Chem. Phys.* **1999**, 110, 8943–8953.
- (16) Bourissou, D.; Guerret, O.; Gabbaï, F. P.; Bertrand, G. *Chem. Rev.* **2000**, 100, 39–92.
- (17) For an example of a silylene with a triplet ground state, see: Sekiguchi, A.; Tanaka, T.; Ichinohe, M.; Akiyama, K.; Tero-Kubota, S. *J. Am. Chem. Soc.* **2003**, 125, 4962–4963.
- (18)  $\text{Sn}\{\text{N}(\text{SiMe}_3)_2\}_2$  is reported to be unreactive towards dihydrogen.<sup>5a</sup>
- (19) Consistent with the relative inertness of **2** compared to **1** with respect to oxidative bond formation, [4 + 1] cycloaddition with 2,3-dimethylbutadiene proceeds only under more forcing conditions for **2**. Thus, while both systems generate stanna-cyclopentene complexes of the type  $\{(\text{MeCCH}_2)_2\text{Sn}(\text{X})\{\text{B}(\text{NDippCH})_2\}$  [X = N(SiMe<sub>3</sub>)Dipp or B(NDippCH)<sub>2</sub>], the reaction in the case of **1** proceeds in <5 min at room temperature,<sup>20</sup> while that for **2** requires stirring for 2 h (see SI).
- (20) Protchenko, A. V.; Dange, D.; Blake, M. P.; Schwarz, A. D.; Jones, C.; Mountford, P.; Aldridge, S. *J. Am. Chem. Soc.* **2014**, 136, 10902–10905.
- (21) Similar structural observations have been made by Power and Ragona on P–H oxidative addition at a diarylstannylene.<sup>6c</sup>
- (22) The first example of dihydrogen activation by a main group system at ambient temperature/pressure was reported as late as 2005: (a) Spikes, G. H.; Fettingter, J. C.; Power, P. P. *J. Am. Chem. Soc.* **2005**, 127, 12232–12233. For other examples of H<sub>2</sub> activation by Group 14 alkylne analogues, see ref 7 and (b) Li, J.; Schenk, C.; Goedecke, C.; Frenking, G.; Jones, C. *J. Am. Chem. Soc.* **2011**, 133, 18622–18625.
- (23) For H<sub>2</sub> activation by main group FLPs, see: (a) Welch, G. C.; San Juan, R. R.; Masuda, J. D.; Stephan, D. W. *Science* **2006**, 314, 1124–1126. (b) Stephan, D. W.; Erker, G. *Angew. Chem., Int. Ed.* **2010**, 49, 46–76.
- (24) For H<sub>2</sub> activation by carbenes, see ref 3 and Frey, G. D.; Lavallo, V.; Donnadiu, B.; Schoeller, W. W.; Bertrand, G. *Science* **2007**, 316, 439–441.
- (25) For H<sub>2</sub> activation by silylenes, see refs 9a and 11.
- (26) For previous reports of Si–H and B–H bond activation by carbenoids, see, for example: (a) C: Frey, G. D.; Masuda, J. D.; Donnadiu, B.; Bertrand, G. *Angew. Chem., Int. Ed.* **2010**, 49, 9444–9447. (b) Al: Chu, T.; Korobkov, I.; Nikonov, G. I. *J. Am. Chem. Soc.* **2014**, 136, 9195–9202.
- (27) The reactivity of **1/2** towards C–H containing substrates has also been probed. The reaction with phenylacetylene, PhCCH, can be shown to proceed not via C–H activation, but via insertion of the C≡C triple bond into both Sn–B linkages (formal stannaboration) to yield a divinylstannylene featuring a pair of pendant borane functions: (a) Protchenko, A. V.; Blake, M. P.; Schwarz, A. D.; Jones, C.; Mountford, P.; Aldridge, S. *Organometallics* **2015**, 34, 2126–2129. See also: (b) Pluta, C.; Pörschke, K.–R. *J. Organomet. Chem.* **1993**, 453, C11–C12.
- (28) Cordero, B.; Gómez, V.; Platero-Prats, A. E.; Revés, M.; Echeverría, J.; Cremades, E.; Barragán, F.; Alvarez, S. *Dalton Trans.* **2008**, 2832–2838.
- (29) Riddlstone, I. M.; Abdalla, J. A. B.; Aldridge, S. *Adv. Organomet. Chem.* **2015**, 63, 1–38.
- (30) The first example a transition metal system capable of effecting the oxidative addition of NH<sub>3</sub> to give M–H and M–NH<sub>2</sub> functions was reported only in 2005: Zhao, J.; Goldman, A. S.; Hartwig, J. F. *Science* **2005**, 307, 1080–1082.
- (31) Haggin, J. *Chem. Eng. News* **1993**, 71, 23–27.
- (32) For previous studies of the reactivity of group 14 carbene-like species towards ammonia, see refs 3, 5, 24, 26b and: (a) Jana, A.; Schulzke, C.; Roesky, H. W. *J. Am. Chem. Soc.* **2009**, 131, 4600–4601. (b) Jana, A.; Objartel, I.; Roesky, H. W.; Stalke, D. *Inorg. Chem.* **2009**, 48, 798–800. (c) Meltzer, A.; Inoue, S.; Präsang, C.; Driess, M. *J. Am. Chem. Soc.* **2010**, 132, 3038–3046. (d) Wang, W.; Inoue, S.; Yao, S.; Driess, M. *Organometallics* **2011**, 30, 6490–6494. For related chemistry of Group 13 systems, see, for example: (e) Zhu, Z.; Wang, X.; Peng, Y.; Lei, H.; Fettingter, J. C.; Rivard, E.; Power, P. P. *Angew. Chem., Int. Ed.* **2009**, 48, 2031–2034. See also: (f) Präsang, C.; Stoelzel, M.; Inoue, S.; Meltzer, A.; Driess, M. *Angew. Chem., Int. Ed.* **2010**, 49, 10002–10005.
- (33) Cardin, C. J.; Cardin, D. J.; Constantine, S. P.; Drew, M. G. B.; Rashid, H.; Convery, M. A.; Fenske, D. *J. Chem. Soc., Dalton Trans.* **1998**, 2749–2756.
- (34) For a related mode of coordination/activation of hydrazine at Ge<sup>II</sup>, see: Brown, Z. D.; Guo, J.-D.; Nagase, S.; Power, P. P. *Organometallics* **2012**, 31, 3768–3772.
- (35) See: Mkhallid, I. A. I.; Barnard, J. H.; Marder, T. B.; Murphy, J. M.; Hartwig, J. F. *Chem. Rev.* **2010**, 110, 890–931 and references therein.
- (36) Alberto, M. E.; Russo, N.; Sicilia, E. *Chem. - Eur. J.* **2013**, 19, 7835–7846.